

Ink and Substrate Compatibility for Electrochemical Sensing in Paper-based Devices

by
Caitlin Reid

A THESIS

submitted to

Oregon State University

Honors College

in partial fulfillment of
the requirements for the
degree of

Honors Baccalaureate of Science in Bioengineering
(Honors Scholar)

Presented November 19, 2019
Commencement June 2020

AN ABSTRACT OF THE THESIS OF

Caitlin Reid for the degree of Honors Baccalaureate of Science in Bioengineering presented on November 19, 2019. Title: Ink and Substrate Compatibility for Electrochemical Sensing in Paper-based Devices.

Abstract approved: _____

Elain Fu

Electrochemical sensing provides a quantitative alternative to colorimetric reactions within paper-based devices. The paper-based devices were fabricated by screen printing the conductive and reference inks onto porous substrates that were evaluated using cyclic voltammetry. Devices were evaluated based on the magnitude of the average anodic peak height, which correlates with a higher signal received from the electrode system, and the coefficient of variation, which correlates with the reproducibility of the devices. The first set of studies compared two conductive carbon ink solvents, two silver ink solvents, and two substrates. The Whatman cellulose, the organic-based solvent carbon ink, and the organic-based solvent silver ink was the most optimal combination with the second highest magnitude of the average anodic peak height ($5.61\mu\text{A}$) with the smallest coefficient of variation (4.47%). A shelf life study was conducted on this ink and material combination to determine the effect that storage time had on the electrode system. Even though there was not a statistically significant change in the signal produced and the time after fabrication, due to the limited number of replications on the later days, a shelf life of seven days was supported.

Key Words: Point-of-care, electrochemical sensing, electrode system, cyclic voltammetry, voltammogram, ink, substrate, anodic peak height, coefficient of variation

Corresponding e-mail address: reidcai@oregonstate.edu

©Copyright by Caitlin Reid
November 19, 2019

Ink and Substrate Compatibility for Electrochemical Sensing in Paper-based Devices

by
Caitlin Reid

A THESIS

submitted to

Oregon State University

Honors College

in partial fulfillment of
the requirements for the
degree of

Honors Baccalaureate of Science in Bioengineering
(Honors Scholar)

Presented November 19, 2019
Commencement June 2020

Honors Baccalaureate of Science in Bioengineering project of Caitlin Reid presented on November 19, 2019.

APPROVED:

Elain Fu, Mentor, representing School of Chemical, Biological, and Environmental Engineering

Joe Baio, Committee Member, representing School of Chemical, Biological, and Environmental Engineering

Adam Higgins, Committee Member, representing School of Chemical, Biological, and Environmental Engineering

Toni Doolen, Dean, Oregon State University Honors College

I understand that my project will become part of the permanent collection of Oregon State University, Honors College. My signature below authorizes release of my project to any reader upon request.

Caitlin Reid, Author

Table of Contents

Chapter One – Introduction	1
<i>Point-of-care Devices</i>	1
<i>Paper-based Microfluidic Devices</i>	2
<i>Commercially Available Device – Pregnancy Test</i>	4
<i>Electrochemical Sensing</i>	5
<i>Commercially Available Device – Blood Glucose Detection</i>	5
<i>Cyclic Voltammetry</i>	6
<i>Screen Printed Carbon Electrodes</i>	8
<i>Summary of Thesis</i>	11
Chapter Two – Material Compatibility	12
<i>Introduction</i>	12
<i>Methods and Materials</i>	13
<i>Materials and Inks Used</i>	13
<i>Cyclic Voltammetry Testing</i>	13
<i>Card Fabrication</i>	13
<i>Detection Methods</i>	15
<i>Results and Discussion</i>	16
<i>Study 1: Organic - Based vs. Water – Based Conductive Carbon Ink with Organic - Based Reference Silver Ink on Nitrocellulose</i>	16
<i>Study #2: Organic-Based vs. Water-Based Reference Silver Ink with Water-Based Conductive Carbon Ink on Nitrocellulose</i>	19
<i>Study #3: Organic-Based vs. Water-Based Conductive Carbon Ink with Organic-Based Reference Silver Ink on Whatman Cellulose</i>	21
<i>Conclusion</i>	23
<i>Methods and Materials</i>	27
<i>Materials and Inks Used</i>	27
<i>Cyclic Voltammetry Testing</i>	28
<i>Card Fabrication</i>	28
<i>Detection Methods</i>	29
<i>Results and Discussion</i>	30
<i>Commercial Electrode System</i>	30
<i>Day Zero and Day One</i>	31
<i>Day Three and Day Seven</i>	31
<i>Day Fourteen and Day Twenty-Eight</i>	32
Chapter 4 – Conclusions and Next Steps	36
<i>Summary of Conclusions</i>	36
<i>Next Steps</i>	38
<i>Extending Shelf Life Study</i>	38
<i>More Robust Screen-Printing Process</i>	38
<i>Development of a Compact Potentiostat and Cyclic Voltammetry System</i>	38
Appendix 1 – Organic-Based Conductive Carbon Ink with Organic-Based Silver Reference Ink on Nitrocellulose (Results from 1/16/18)	40

<i>Appendix 3 – Organic-Based vs. Water-Based Conductive Carbon Ink with Organic-Based Silver Reference Ink on Whatman Cellulose (Results from 1/23/18)</i>	45
<i>Appendix 4 – Shelf Life Study</i>	47
<i>Day Zero</i>	47
<i>Day One:</i>	48
<i>Day Three:</i>	49
<i>Day Seven:</i>	50
<i>Day Fourteen:</i>	51
<i>Day Twenty-Eight:</i>	53
<i>References</i>	54

Chapter One – Introduction

Point-of-care Devices

Point-of-care (POC) devices are a popular alternative to laboratory-based testing within the medical field. Laboratory-based tests are expensive, require electricity, training, and proper instrumentation, and take several weeks to receive results. The advantage of clinical testing is the results are typically quantitative and highly sensitive. Point-of-care devices are designed to be user friendly and require minimal-to-no medical training, electricity, or instrumentation. These devices are cheap to produce, and results are obtained rapidly (Betancur, 2017). There has been a growing platform for point-of-care devices for their capability to perform existing laboratory-based assays in low resource settings (Yetisen, 2013). Figure 1 represents various applications for point-of-care devices beyond the typical clinical diagnostics.

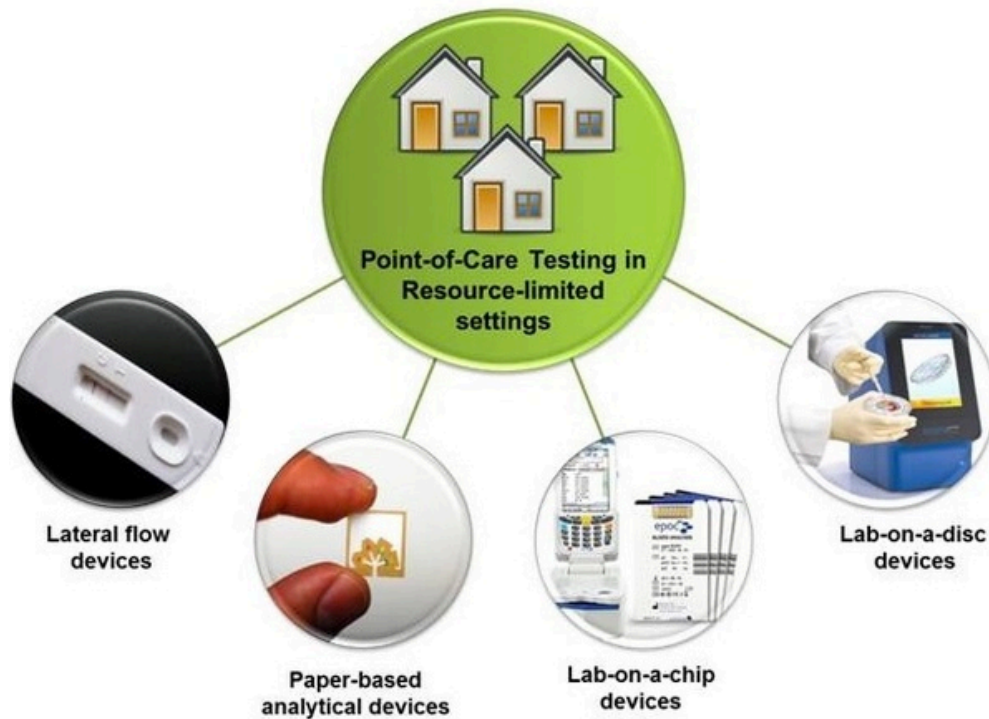


Figure 1: Point-of-care devices provide an alternative testing method to the typical laboratory-based testing (Renub, 2018).

Paper-based Microfluidic Devices

One major type of point-of-care devices are paper-based microfluidic devices. These devices are popular because they require a small sample volume and allow rapid mass transport due to the small channels. Microfluidic devices can be fabricated on paper making them less expensive to produce while also keeping them portable and compact. Paper-based microfluidic devices have provided an inexpensive, reproducible, and disposable format for diagnostic testing that have the capability to be produced in mass quantities (Hu, 2014). They require no external instrumentation as the fluid movement through porous materials is driven by capillary flow. Porous materials are made of thousands of small capillaries that help to facilitate the movement of fluid. Understanding flow on a nanoscale is critical for fluid movement through porous materials (Dimitrov, 2007). The Washburn equation (Equation 1) describes the rate that fluid flows through a single cylindrical capillary.

Equation 1: Lucas-Washburn Equation (Washburn, 1921) describes fluid flow through a capillary.

$$L = \sqrt{\frac{\gamma r \cos \theta t}{2\mu}}$$

Where L is the distance that the capillary, γ is surface tension, r is the pore radius, t is time, θ is the contact angle, and μ is the viscosity.

Capillary action occurs when the adhesive forces (solid-liquid interactions) are stronger than the cohesive forces (liquid-liquid interactions) (Peiris, 2019). This provides an explanation for why fluids travel up a thin cylinder or through a porous material such as a paper towel. Figure 2 provides a schematic for the forces involved within capillary action.

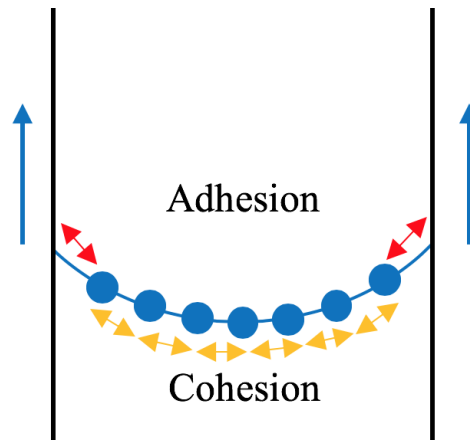


Figure 2: Liquid travels up the walls of the thin cylinder as the adhesive forces are stronger than the cohesive forces. This phenomenon is referred to as capillary action and is the driving force for sample movement within a paper-based microfluidic device.

One popular form of paper-based microfluidic devices are lateral flow tests (Betancur, 2017). These tests utilize components such as cellulose and nitrocellulose, along with other porous materials, to enable fluid to flow through the assay. A lateral flow test immunoassay typically relies on a colorimetric readout, which results from the interaction between the analyte (desired component of the sample taken) and a tagged detection antibody (Cheng, 2015). Antibodies are typically tagged with a colored molecule such as a gold nanoparticle which allows it to be visualized by the naked eye. Immobilized capture antibodies, which are pre-dried on the substrate, also interact with the analyte when it is present in the sample. If the desired analyte is present, this interaction produces a bright color, otherwise, no color is observed. A schematic of the antibody-antigen complex is shown in Figure 3.

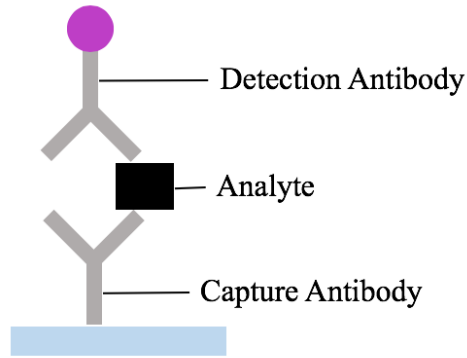


Figure 3: A sandwich assay (Cheng, 2015) between a tagged detection antibody (such as a gold nanoparticle) and the immobilized capture antibody. This produces a colorimetric reaction when the captured analyte is present, which can be visualized by the naked eye.

Commercially Available Device – Pregnancy Test

One common example of a lateral flow device is a pregnancy test (Cheng, 2015). This device can be used at home with no medical training and will provide results in under five minutes at a unit cost of less than \$5. Once urine contacts the sample pad, it travels down the length of the device to the test line and the control line. If a woman is pregnant, the analyte will be captured between the detection and capture antibodies creating the sandwich assay. The urine will also hydrate the control line to verify that the immunoassay is valid. A schematic of a lateral flow device is shown in Figure 4.

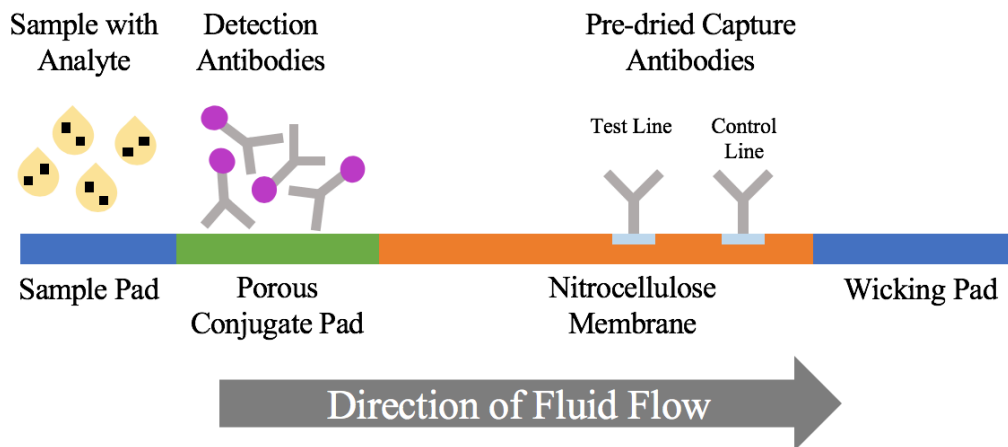


Figure 4: Side view of a lateral flow device which utilizes a sandwich antibody assay to detect the presence a specific analyte within a sample. This immunoassay produces

a colorimetric reaction on the test and control lines representing the presence or absence of the desired analyte (Cheng, 2015).

Electrochemical Sensing

Although there are many advantages to paper-based lateral flow devices, they lack sensitivity and can only be utilized for qualitative (yes/no or presence/absence) or semi-quantitative (low/medium/high) readouts. Some semi-quantitative readouts utilize colorimetric reactions by quantifying the amount of color change (faint color is low concentration while vibrant color is high concentration). One potential way to advance this approach is to utilize a cell phone or a camera to quantify the color change that occurs within the devices (Wang, 2011). An alternative to colorimetric reactions altogether would be to use electrochemical sensing which provides a numerical value to the reactions (Hu, 2014). The electrochemical sensing method used within this thesis is an amperometric sensor. These sensors measure the current response to detect the concentration of an analyte at a fixed potential (Zhang, 2014). The current strength is dependent on the concentration of the electrolyte solution (Price, 2019). The electrochemical sensing platform can be integrated within a microfluidic device by fabricating the electrode system on a paper-based device. Such devices can detect for nucleic acids, alcohol, uric acid, cholesterol, lactate, and glucose (Vanshist, 2015). This allows for a cost-effective testing device that can provide rapid results in the comfort of the user's home.

Commercially Available Device – Blood Glucose Detection

One example of an electrochemically sensing diagnostic device is a blood glucose meter. Blood glucose is related to the production and management of the hormone Insulin which allows muscles, fat, and liver cells to absorb glucose from the blood and use it for energy. An individual's blood glucose levels are easy to detect using a simple at home glucometer, a drop of blood, and a test strip. The test strip contains glucose oxidase, which is an enzyme that produces an electrical signal when it reacts with the glucose in the blood (Jensen, 2011). The strength of this electrical signal from the reaction is displayed on the glucometer's readout window, communicating the results. A schematic of the process can be seen in Figure 5.

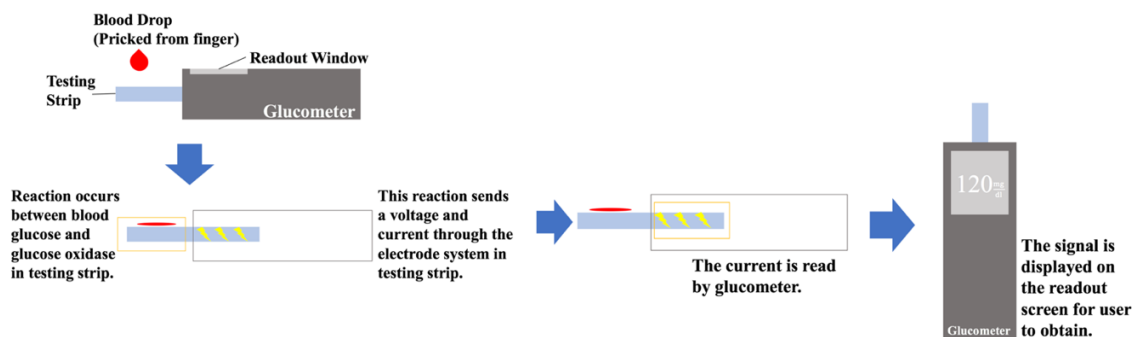


Figure 5: A blood drop is placed onto a testing strip that contains the enzyme glucose oxidase. The reaction sends an electrical signal into the glucometer which is read by the two-electrode system and displays results in the readout window.

Cyclic Voltammetry

Cyclic voltammetry (CV) is an electrochemical sensing technique that investigates the oxidation and reduction reaction that occurs in molecular species (Elgrishi, 2017). For this study, a ferrocenemethanol (FCM) solution was used as the electrolyte solution (Fig. 6).

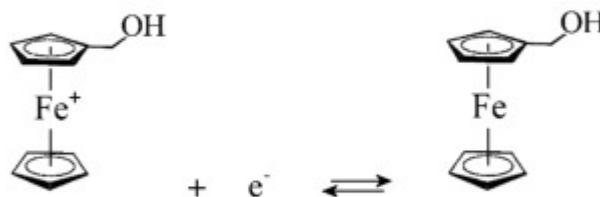


Figure 6: Structure of the ferrocenemethanol molecule in its reduced and oxidized state (Montiel, 2017).

The transfer of the electron to and from the FCM molecule occurs as it favors a lower energy system for an applied voltage. When an external power source (such as a potentiostat) applies a voltage to the electrodes, the electrode can modulate the energy of the electrons and produce a current which is read by the power source. Cyclic voltammetry produces a graph traces called voltammograms (Fig. 7), where the applied voltage and the resulting current are on the x and y axis respectively (Elgrishi, 2017).

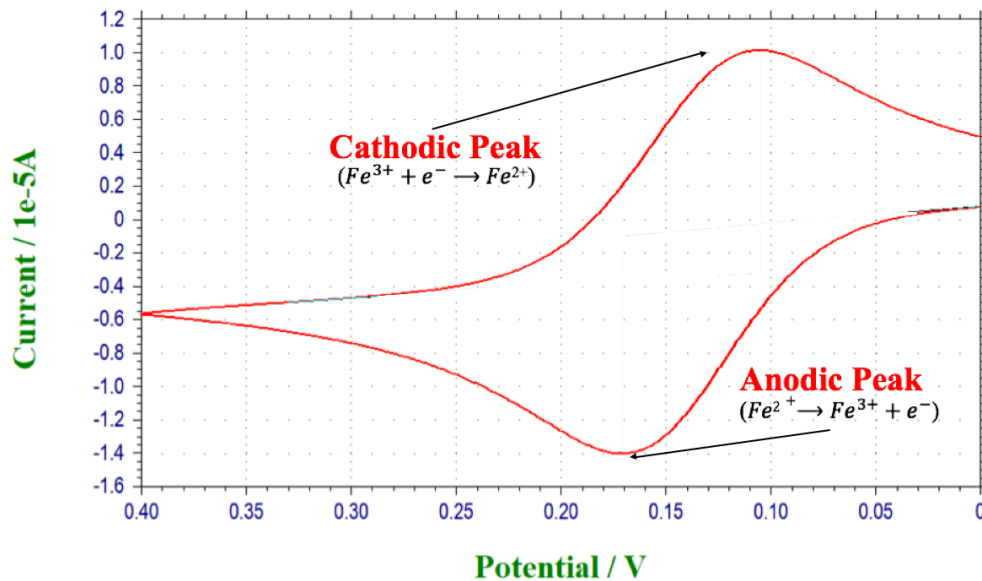


Figure 7: Voltammogram that is produced when voltage from an external source is applied to an electrode system and a current is produced.

For a reversible reaction, which can undergo both oxidation and reduction, the typical voltammogram follows the same pattern as above with two peaks. For this thesis, an initial voltage of zero volts was applied to the system and increased to 0.4V at a scan rate of 25mV/sec. As the voltage increases, Fe^{2+} molecules travel to the electrode surface, where an electron is removed from the molecule oxidizing it to its Fe^{3+} form. The anodic peak height occurs when the rate at which oxidation is occurring is at its peak (lowest current). As voltage is continually applied, the current decreases until the potentiostat reverses the direction at which the voltage is applied (0.4V throughout this study). As the voltage decreases, Fe^{3+} molecules travel back to the electrode surface where an electrode is attached to the molecule, reducing it to its Fe^{2+} form. The cathodic peak height occurs when the rate at which reduction is occurring is at its peak (highest current). Once the voltage reaches zero volts, the scan completes, and another scan is initiated. In this thesis, seven total scans were completed. For analysis purposes, only the last six scans were used during analysis.

Cyclic voltammetry and the voltammogram is modeled using the Randles-Sevick equation (Aliabali, 2010), seen in Equation 2. This equation describes the various components that effect the peak current and helps identify the anodic and cathodic peak

heights. The peak currents were calculated within the CHI software and exported for analysis.

Equation 2: Randles-Sevick Equation (Aliabali, 2010) describes the effect of scan rate on the peak current and allows for the identification of the anodic and cathodic peak heights.

$$i_p = 0.4462nFAC \left(\frac{nFvD}{RT} \right)^{\frac{1}{2}}$$

Where i_p = current (amps), n = number of electrons transferred in the redox event (usually 1), A = electrode area (cm^2), F = Faraday Constant (C mol^{-1}), D = diffusion coefficient (cm^2/s), C = concentration (mol/cm^3), v = scan rate (V/s), R = gas constant ($\text{J K}^{-1} \text{mol}^{-1}$), T – temperature (K).

The Randles-Sevick equation shows that peak height is dependent on several different components within the electrode system. The most important component during this study was the electrode area. If there is a larger surface on which the redox reaction can occur, it will produce a larger current and a larger magnitude of the peak height. When the ink penetrates the substrate too deeply (the ink disintegrates the substrate during fabrication), it produces higher magnitude peak heights because it increases the surface area on which the reaction can occur. This is undesirable because the penetration level (how much of the substrate disintegrates) varies across devices, reducing the reproducibility. Each study, therefore, evaluates the devices based on both the magnitude of the anodic peak heights as well as the coefficients of variation. This shows which devices provide the maximum magnitude of signal most consistently.

Screen Printed Carbon Electrodes

Throughout this thesis, a three electrode system was used for the electrochemical sensing device. A three-electrode system uses a working, counter, and reference electrode. A voltage is applied to the system by an amperometric sensor (potentiostat) and electrons flow through working electrode. As a voltage is applied to the working electrode, an opposite voltage is applied to the counter electrode to keep the system balanced. The reference electrode has an established electrode potential to compare to the working electrode's activity (Bacher, 2003). In a laboratory electrode system, the

three electrodes rest in the electrolyte solution that contains the molecular species experiencing oxidation and reduction (Fig. 8).

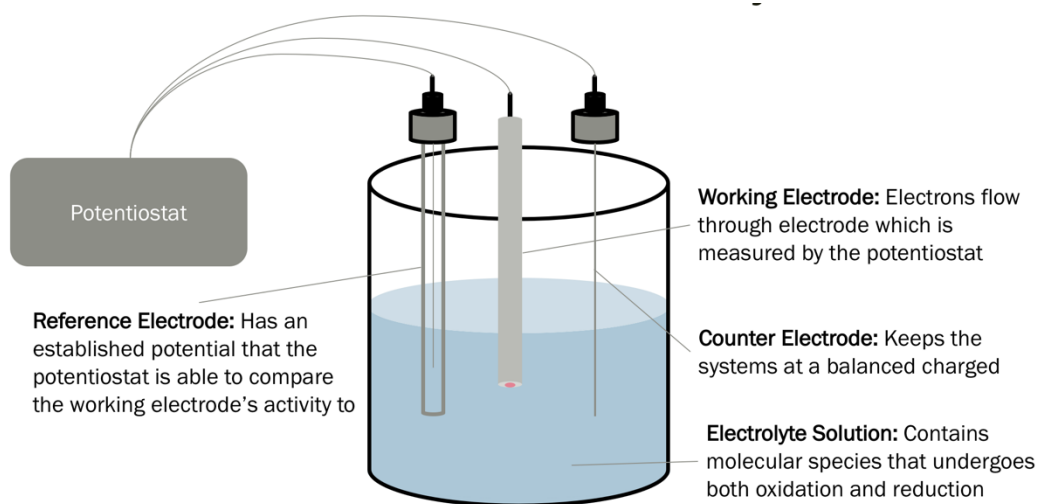


Figure 8: Laboratory setup of a three-electrode system that includes a working, counter, and reference electrode connected to a potentiostat and placed into an electrolyte solution.

An alternative to a three-electrode system is one that contains only two electrodes. In a two-electrode system, the counter and the working electrode are combined and the potential is applied across both electrodes. The current is measured from the combined working and counter electrodes and compared to that of the reference electrode. Measuring this current can affect the applied potential therefore these systems are not as reliable. Because of the reliability issues, a three-electrode system will be used within this thesis.

Because these laboratory systems are bulky, a more compact approach is with a screen-printed electrode system. These systems are fabricated by screen printing the carbon conductive ink and silver reference ink through a patterned stencil onto paper substrates (Lin, 2004). A screen-printed electrode system contains all three of the same electrodes however the electrolyte solution is added to a wax printed well to allow the transfer of electrons to occur between the working and the counter electrodes (Fig 9). This creates an electrical current that is read and recorded on the potentiostat.

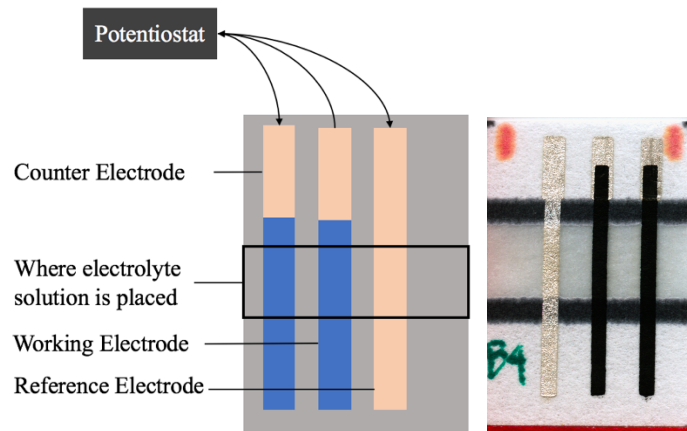


Figure 9: Top view of a screen printed three-electrode system. A schematic of the devices is on the left and an actual device is on the right.

Screen-printed devices contain two ink types. The composition of these inks determines the selectivity and sensitivity for each diagnostic device (Hutanu, 2013). Inks contain three general parts: a filler, a binder, and a solvent (Fletcher, 2016). Fillers are the conductive portion of the ink (carbon and silver), while the binder is nonconductive and connects the filler to the substrate. Once the ink is printed onto the substrate, the solvent evaporates leaving the only the binder and filler. Reference electrodes are typically made of a different ink than the working and counter electrodes. Two common examples of reference systems include mercury mercury-chloride (Hg_2Cl_2) and silver-silver chloride (AgCl) (Devengenzo, 2007).

Fabrication of these devices is a simple procedure. The substrate (typically Mylar, Whatman paper, or cloth depending on the application of the test) is placed inside of a holder which stabilizes the substrate during the screen-printing process (Fig. 10). A stencil, generally a very thin piece of Mylar with the design of the reference ink, is taped on top of the holder. Well mixed reference ink is then placed on top of the screen at the top of the design. A squeegee is dipped into the ink and is moved down the length of the device pressing the ink into the stenciled design. The substrate is removed from the holder and placed into an oven for an expedited drying process. This same procedure is repeated using a different design screen for the conductive carbon ink in order to produce the final product.

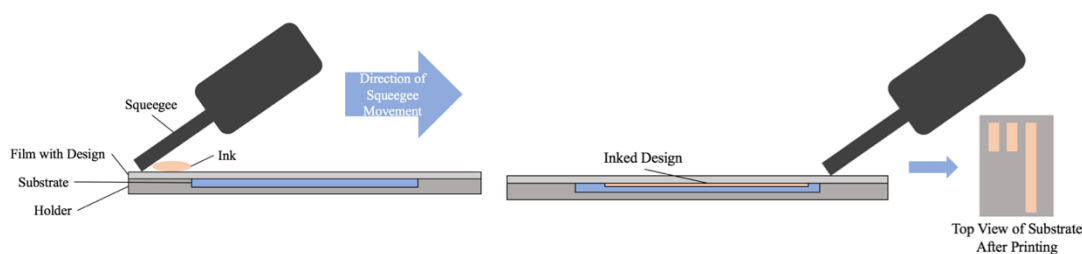


Figure 10: Fabrication of screen-printed electrodes involves a holder, substrate, design film, squeegee and ink. A simple motion will imprint the design onto the plastic resulting in the final design.

Summary of Thesis

This thesis investigated improving and optimizing the signal produced within an electrochemical sensing paper-based diagnostic device. Studies were evaluated based on the magnitude of the average anodic peak height and the coefficient of variation obtained through cyclic voltammetry. A larger anodic peak height correlates with a higher signal received from the electrode system, and a low coefficient of variation correlates with reproducibility of the devices.

Chapter Two evaluated the compatibility of two conductive carbon inks, two silver reference inks, and two substrates when utilized in an electrochemical sensing system. The carbon and silver inks differed in their solvent type as each had both an organic-based solvent and a water-based solvent. Each carbon ink and silver ink was characterized on both nitrocellulose and Whatman cellulose for substrate comparisons. Chapter Three determined the effects of storage time on screen-printed carbon electrodes. This study leveraged the most optimal pairing determined in Chapter Two. The shelf life study lasted twenty-eight days with testing occurring at various time points throughout.

Chapter Two – Material Compatibility

Introduction

In order to produce the most efficient electrical sensor, it was important to maximize the magnitude of the anodic peak heights obtained during a CV. This study aimed to determine which combination of carbon ink solvent, silver ink solvent, and substrate produced the largest magnitude of the average anodic peak height with the smallest coefficient of variation.

This study compared two carbon inks, two silver inks, and two substrates. Both the carbon and silver inks differed based on the type of solvent, one containing an organic-based solvent (non-polar) and the other a water-based solvent (polar). Previous studies conducted within the lab utilized the organic-based solvent inks, so it was desired to observe the difference that solvent chemistry (polar vs. non-polar) had on the signal produced. The two tested substrates were nitrocellulose and Whatman cellulose. Nitrocellulose is commonly used in paper-based microfluidic devices due to its ability to adhere antibodies to the surface. As a lab group interested in advancing immunoassays, fabricating the devices on a substrate with a higher absorbance to antibodies had the potential to increase the magnitude of the average anodic peak height. Whatman cellulose is another common substrate used in point-of-care devices due to its low cost. Ferrocenemethanol (FCM) was the electrolyte solution used for all devices as it is a model solution for electrode systems. The pairings tested throughout all three studies are shown in Table 1.

Table 1: Carbon ink solvent, silver ink solvent, and substrate pairings for determining the most optimal material combination for use in an electrode system

Study	1		2		3	
Carbon Ink Solvent	Organic - Based	Water – Based	Water - Based		Organic - Based	Water - Based
Silver Ink Solvent	Organic – Based		Organic - Based	Water - Based	Organic - Based	
Substrate	Nitrocellulose		Nitrocellulose		Whatman Cellulose	

Methods and Materials

Materials and Inks Used

This study compared two carbon inks, two silver inks, and two substrates in screen-printed devices. The carbon and silver inks included an organic-based solvent ink (Gwent), and a water-based solvent ink (Creative Materials). Substrates include Whatman cellulose (EMD Millipore) and nitrocellulose (EMD Millipore). Ferrocenemethanol (EMD Chemicals) was the electrolyte solution used during testing. Fabrication of devices included 10-mil Mylar backing (Tekra), 1-mil Mylar screens (Tekra), and a squeegee. Devices were designed with Draftsight (Dassault Systems) and materials were cut with a CO2 laser (Universal). A wax printer (Xerox ColorCube) and an oven (Thermo Fisher) were utilized for defining a well area. CV scans were performed using a potentiostat and macro functions (CH Instruments).

Cyclic Voltammetry Testing

The signal was read from the potentiostat and saved as a macro file within the Electrochemical software. The macro files were analyzed using a custom MATLAB (Natick) program which exported data into an Excel (Microsoft) file. All values and peak heights were determined through the CHI software. These values were graphed and compared based on the magnitude of the anodic peak heights and coefficients of variation. The coefficient of variation was calculated using Equation 3.

Equation 3: Calculation of the coefficient of variation using the average and standard deviation of the magnitude of the anodic peak heights from the MATLAB script. The average and standard deviations were calculated using an Excel formula.

$$\text{Coefficient of Variation} = \left| \frac{\text{Stdev}}{\text{Average}} \right| * 100$$

Card Fabrication

Card fabrication varied based on the substrate used. Mylar aspects were printed and used for both substrates including a holder, a silver stencil, and a carbon stencil.

Nitrocellulose

In addition to the Mylar holder and stencils, a Mylar backing for the nitrocellulose devices was printed to add more stability during baking and testing. Wax transfer printing was used to transfer the wax well area to the nitrocellulose (Downs, 2018). This involved printing the well area onto 2-mil transparent Mylar sheet using the wax printer and overlaying the wax sheet on top of the nitrocellulose substrate, using clamps and glass plates to ensure consistent and constant pressure. The glass plates and clamps were then baked at 100°C for 15 minutes. The silver stencil was taped on top of the substrate holder with the nitrocellulose device inside and well mixed silver reference ink was placed at the top of the design. A designated silver squeegee was pulled down the length of the Mylar stencil with constant pressure to imprint the design onto the substrate after which the card was then baked at 100°C for ten minutes. After removing the silver stencil, the carbon stencil was taped on top of the substrate holder and well mixed carbon ink was placed at the top of the design and pulled down with a squeegee. The water-based solvent carbon ink was printed first followed by the printing of the organic-based solvent ink with a new stencil and squeegee quickly after. The cards were then placed in the oven at 100°C for ten minutes. After the baking period, the cards were cut into six individual devices which were then ready for testing.

Whatman Cellulose

For Whatman cellulose devices, Whatman was wax printed, baked, and cut into cards. The silver stencil was taped on top of the substrate holder with the Whatman device inside. The designated organic-based or water-based silver reference ink was mixed and placed at the top of the design on the silver stencil. A designated silver squeegee was pulled down the length of the Mylar stencil with constant pressure to imprint the silver design onto the substrate. The card was then baked at 100°C for ten minutes. After removing the silver stencil, the carbon stencil was taped on top of the substrate holder. The designated organic-based or water-based carbon ink was mixed and placed at the top of the carbon design and pulled down with a designated organic-based or water-based squeegee to imprint the carbon design onto the substrate. The water-based solvent carbon ink was printed first followed by the printing of the organic-based

solvent ink with a new stencil and squeegee quickly after. The cards were then placed in the oven at 100°C for ten minutes. After the baking period, the cards were cut into six individual devices which were then ready for testing.

Detection Methods

Devices were placed on a stand with a Mylar holder and secured in place using an alligator clip. The three electrodes were placed on their designated connections as seen in Figure 11. The white electrode clipped to the reference electrode, the red electrode clipped to the counter electrode, and the green electrode clipped to the working electrode.

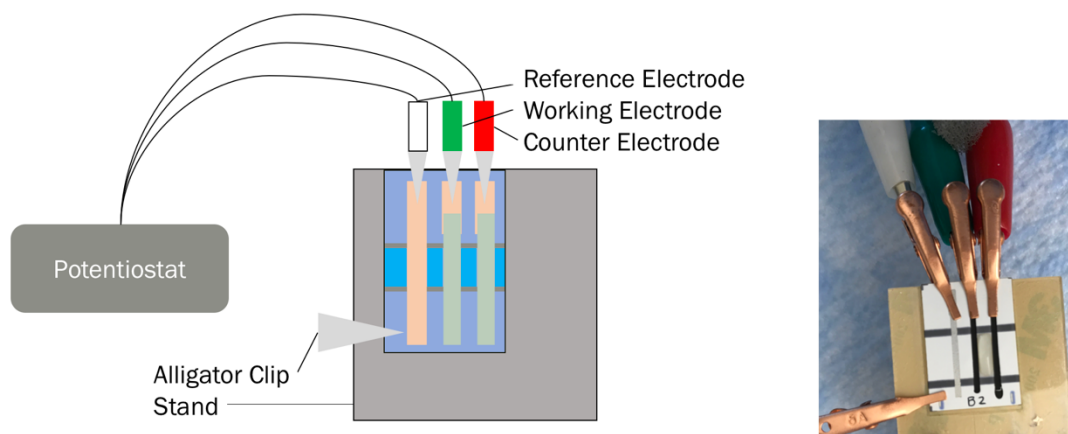


Figure 11: A single nitrocellulose electrochemical sensing device interfacing with CHI potentiostat. A schematic of the setup is on the left with the actual device setup on the right.

The Electrochem software was opened and the scan rate and applied voltage were set. FCM was pipetted into the well space and testing began one minute after, allowing for the well area to fully wet out. After the testing completed the specified number of scans, the devices were disconnected, and the data was imported to MATLAB using a custom-built program to handle text-files.

Results and Discussion

Study 1: Organic - Based vs. Water – Based Conductive Carbon Ink with Organic - Based Reference Silver Ink on Nitrocellulose

The first set of devices compared the organic-based solvent and the water-based solvent carbon inks on the nitrocellulose substrate. The silver ink used during this study contained the organic-based solvent. Two total cards were printed for replicate devices. During this set, 5.63 μ L of 1.35 mM FCM was pipetted into the well area.

Figure 12 shows the average current value of each device type for the voltage applied. In this evaluation, the A series is the organic-based solvent (N=6) and the B series is the water-based solvent (N=5)¹. The average magnitude of the anodic peak heights from each device were averaged for each ink solvent type (Fig. 13). Individual device data can be viewed in Appendix 1.

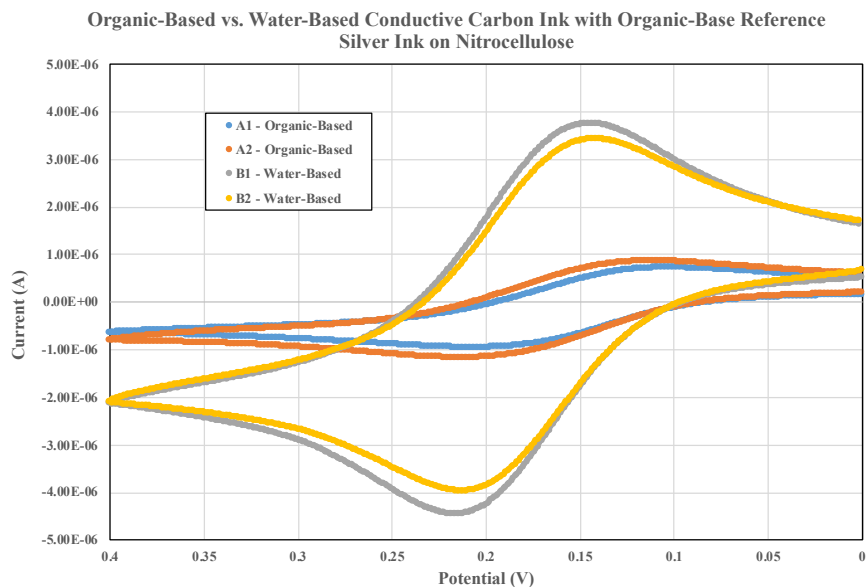


Figure 12: Overall results comparing the organic-based solvent (A series) and water-based solvent (B series) carbon inks on a nitrocellulose substrate. During evaluation, card B12 was excluded from analysis.

¹ Card B12 was excluded from the data as it was hit twice during collection and therefore was not a true representation of the data

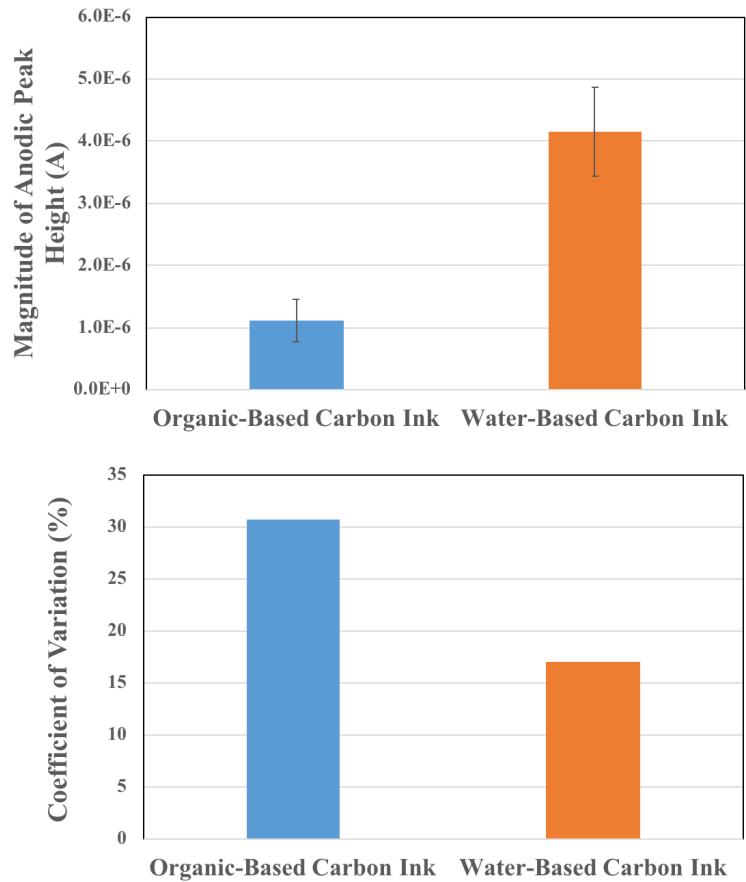


Figure 13: The magnitude of the average anodic peak heights and the coefficient of variation from all devices were averaged for each carbon ink solvent type. The water-based solvent carbon ink had a larger magnitude anodic peak height ($4.15 \pm 0.706 \mu\text{A}$) than the organic-based solvent carbon ink ($1.11 \pm 0.339 \mu\text{A}$). The error bars represent the standard deviation. The water-based solvent carbon ink also had a smaller coefficient of variation (17.0%) than the organic-based solvent carbon ink (30.6%).

On nitrocellulose, with the organic-based solvent silver reference ink, the water-based solvent conductive carbon ink produced a larger average anodic peak value with a smaller coefficient of variation. These scans produced more uniform and consistent scans while also producing a higher magnitude of the anodic peak value, making the combination of the organic-based silver ink with the water-based carbon ink on nitrocellulose the most compatible combination for this device set.

During testing, it was noted that the organic-based carbon ink devices had difficulty wetting out compared to the water-based carbon devices which wet immediately. The

back of the devices was investigated for penetration of the nitrocellulose substrate (Fig 14).

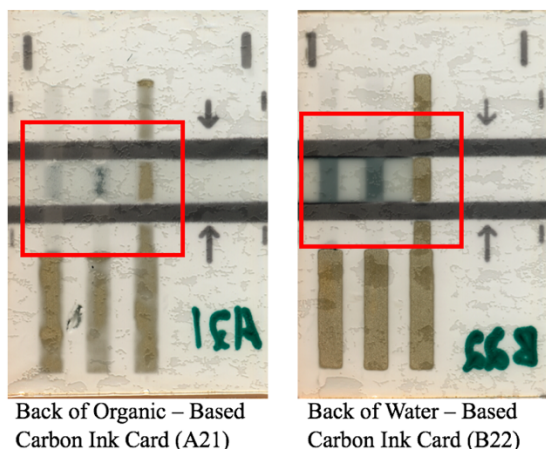


Figure 14: The backs of each of the cards show the ink's penetration into the nitrocellulose devices. The card on the left shows a dry well area with the penetration of the organic-based carbon ink on the middle electrode. This provided a barrier that didn't allow for the FCM to flow through. The card on the right shows a wetted well area where the FCM solution readily traveled under the working and counter electrodes. The organic-based solvent silver ink was used for both cards. This ink deeply penetrated the nitrocellulose substrate and created a boundary which restricted fluid transport. After looking at cross sections of the nitrocellulose devices (Fig. 15), it was noted that the silver ink degraded the nitrocellulose substrate. This degradation allowed a higher magnitude of the anodic peak height because there was a larger surface area of the electrode for molecular oxidation (Eq. 2). This degradation also led to the very high coefficients of variation for this study because it is difficult to replicate. A water-based silver reference ink was ordered to determine if reduced degradation could further improve the scan consistency and maintain the magnitude of the anodic peak heights.

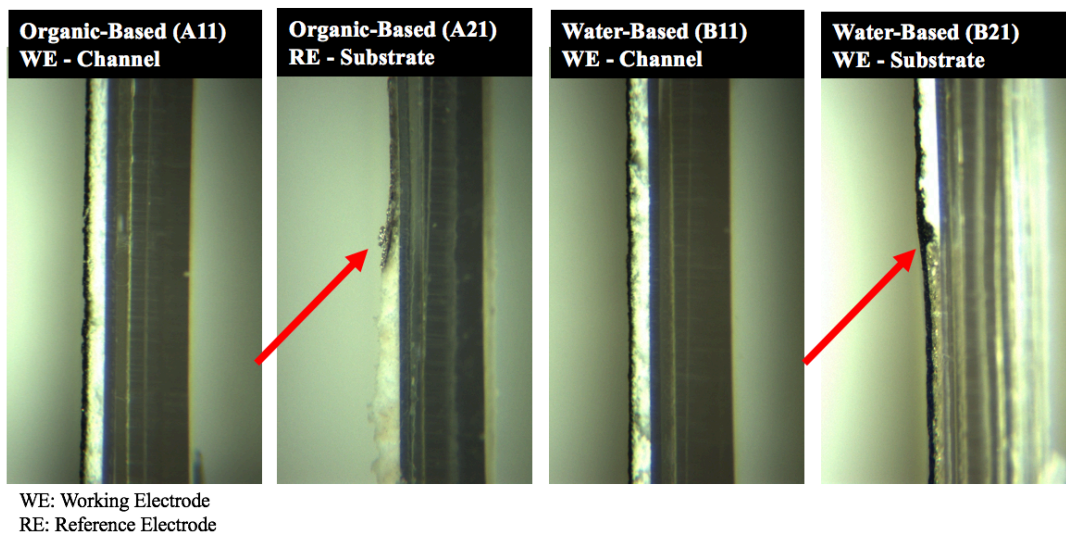


Figure 15: Cross-section images of various devices show the varying degree of substrate degradation of the carbon and silver inks. The deeper penetration restricted fluid flow under the electrodes and prevented a fully wetted well area. This led to high coefficients of variation and less consistent device magnitude of the anodic peak heights.

From the first set of devices, it was concluded that on a nitrocellulose substrate, the water-based solvent conductive carbon ink produced higher magnitude values for the anodic peak height. Additionally, this carbon ink did not degrade the nitrocellulose substrate as much as the organic-based solvent carbon ink.

Study #2: Organic-Based vs. Water-Based Reference Silver Ink with Water-Based Conductive Carbon Ink on Nitrocellulose

The second set of devices used the water-based solvent silver ink recommended after the first study. This set compared the organic-based and the water-based solvent silver inks with water-based carbon ink on the nitrocellulose substrate. Figure 16 shows the average of the magnitude of the average anodic peak heights and the average coefficient of variation from each device for each silver ink solvent type. During this set, 6.75 μ L of 1.35 mM FCM was pipetted into the well area. Individual device data can be viewed in Appendix 2.

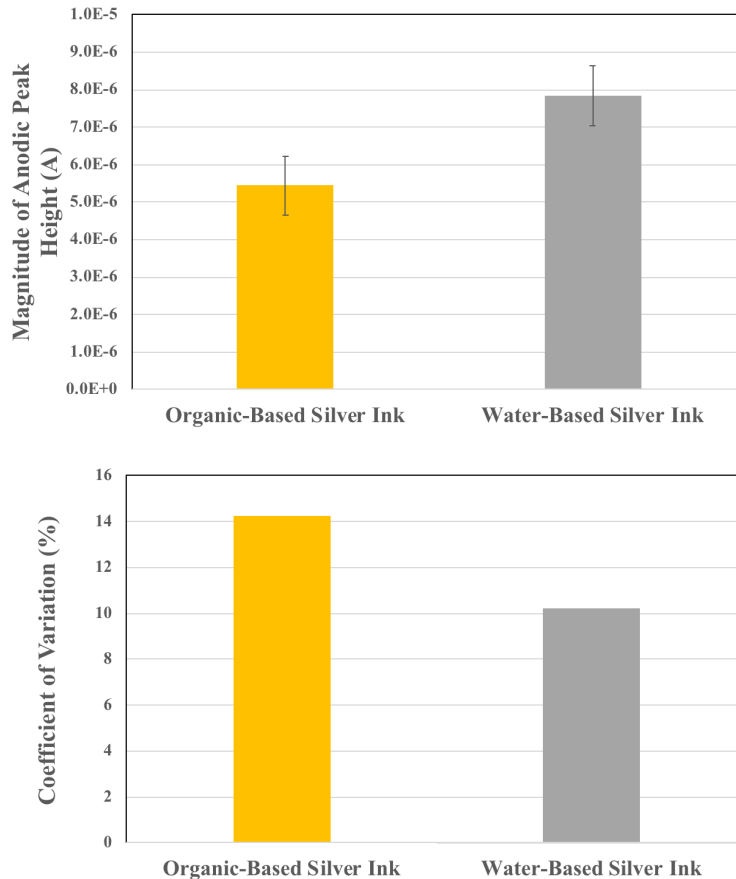


Figure 16: The magnitude of the average anodic peak height and the average coefficient of variation from each device were averaged for each silver ink solvent type. The water-based silver ink had a larger average magnitude anodic peak height ($7.84 \pm 0.801 \mu\text{A}$) than the organic-based silver ink ($5.44 \pm 0.774 \mu\text{A}$) and a smaller coefficient of variation (10.2%) than the organic-based silver ink (14.2%). The error bars represent the standard deviation.

On a nitrocellulose substrate with water-based solvent conductive carbon ink, the water-based solvent silver reference ink produced a larger magnitude of the average anodic peak value. The organic-based solvent silver reference ink had a smaller coefficient of variation. Although the device scans were uniform the scans were not consistent on all devices as the peak heights decreased as the number of scans increased.

From previous experiments, the water-based solvent conductive ink performed well when paired with the organic-based solvent silver reference. These results were not

replicated here. It was expected that the water-based conductive carbon ink paired with the water-based silver would improve results on nitrocellulose due to less penetration of the nitrocellulose substrate. Our results did not support this hypothesis as the scans continued to decrease in the magnitude of the anodic peak heights as time increased.

Study #3: Organic-Based vs. Water-Based Conductive Carbon Ink with Organic-Based Reference Silver Ink on Whatman Cellulose

The third study compared organic-based and water-based solvent carbon inks with organic-based solvent silver ink on the Whatman cellulose substrate. During this set, 10.2 μ L of 1.35 mM FCM was pipetted into the well area. The difference in volume added from the previous set is the fluid capacity of the porous materials.

Figure 17 shows the averaged CV scans for each device carbon ink solvent type (N=3) for the applied voltage. Figure 18 shows the average of the average magnitude of the anodic peak heights and the average coefficient of variation from each device for each ink solvent type. Individual device data can be viewed in Appendix 3.

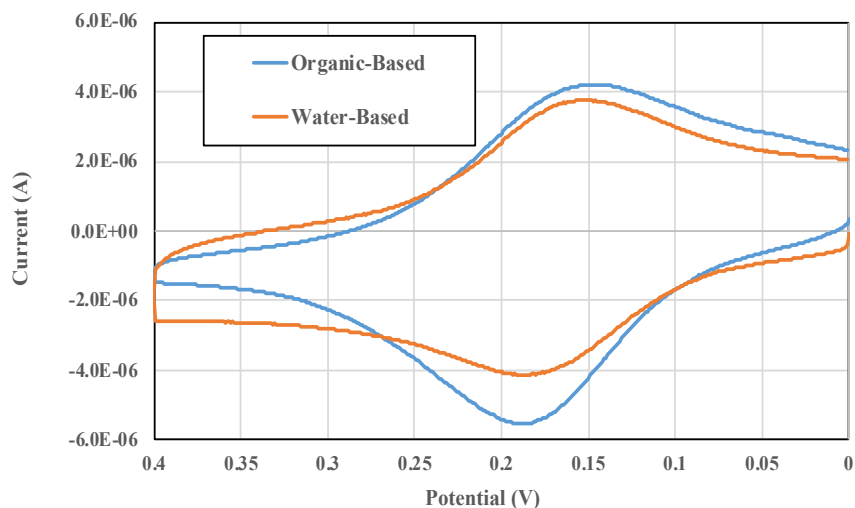


Figure 17: Overall results comparing the organic-based and water-based conductive carbon conductive inks on a Whatman cellulose substrate.

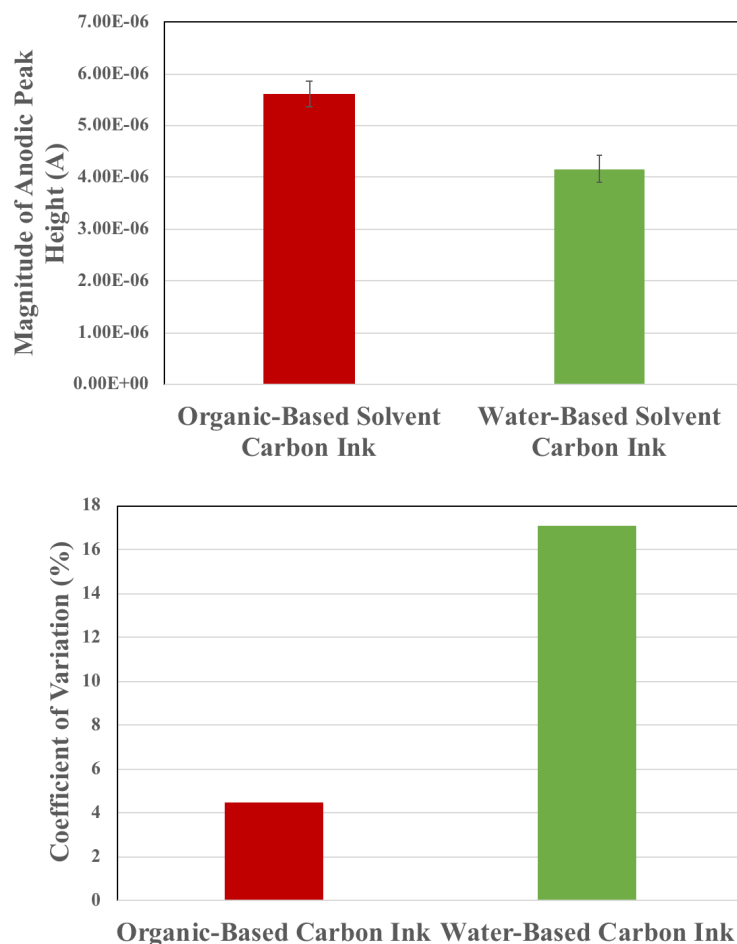


Figure 18: The average magnitude of the anodic peak heights and the average coefficient of variation from each device were averaged for each carbon ink solvent type. The organic-based carbon ink had a larger average magnitude anodic peak height ($5.61 \pm 0.251 \mu\text{A}$) than the water-based carbon ink ($4.16 \pm 0.712 \mu\text{A}$) and a smaller coefficient of variation (4.47%) than the water-based carbon ink (17.1%). The error bars represent the standard deviation.

On Whatman cellulose, with the organic-based solvent silver ink, the organic-based solvent carbon ink produced a larger magnitude of the average anodic peak value with a smaller coefficient of variation, making the pairing between the organic-based solvent carbon ink, organic-based solvent silver ink, and Whatman cellulose the most optimal combination. The low coefficients of variation represent the reduced variability and substrate degradation on the Whatman cellulose.

Conclusion

The purpose of this study was to investigate the compatibility of two substrates, two conductive carbon ink solvents, and two reference silver ink solvents. The devices were compared based on the magnitude of the average anodic peak height and the coefficient of variation. The magnitude of the average anodic peak heights helped to determine the signal of the electrode system and the coefficient of variation helped to determine the reproducibility. These are both important aspects to observe for the end application of paper-based electrochemical sensing devices.

The first study showed that on nitrocellulose with the organic-based silver ink, the water-based carbon ink produced a higher magnitude of the average anodic peak height ($4.15 \pm 0.707 \mu\text{A}$) with a smaller coefficient of variation (17%) than the organic-based carbon ink. After observing the devices, the organic-based solvent inks (both the carbon and the silver inks) had degraded the nitrocellulose substrate. This motivated the use of a water-based solvent silver ink to see if there was less substrate degradation.

The next study showed that on nitrocellulose, the water-based silver reference ink with the water-based carbon ink produced a higher magnitude of the average anodic peak height ($7.84 \pm 0.814 \mu\text{A}$) with a smaller coefficient of variation (10.22%) than the organic-based silver ink. The use of the water-based reference ink did not have the anticipated result as the devices still had a difficult time wetting out completely beyond the electrodes.

The last study showed that on Whatman cellulose with an organic-based silver ink, the organic-based carbon ink produced a higher magnitude of the average anodic peak height ($5.61 \pm 0.251 \mu\text{A}$) with a smaller coefficient of variation (4.47%) than the water-based carbon ink. All the study results can be seen in Table 2 and Figure 19.

Table 2: Overview of all studies completed with the average anodic peak heights and the coefficients of variation.

Study	1		2		3	
Carbon Ink Solvent	Organic-Based	Water-Based	Water-Based		Organic-Based	Water-Based
Silver Ink Solvent	Organic-Based		Organic-Based	Water-Based	Water-Based	
Substrate	Nitrocellulose		Nitrocellulose		Whatman Cellulose	
Average Magnitude Anodic Peak Value (μA)	1.11	4.15	5.44	7.84	5.61	4.16
Coefficient of Variation (%)	30.6	17.0	14.23	10.2	4.47	17.1

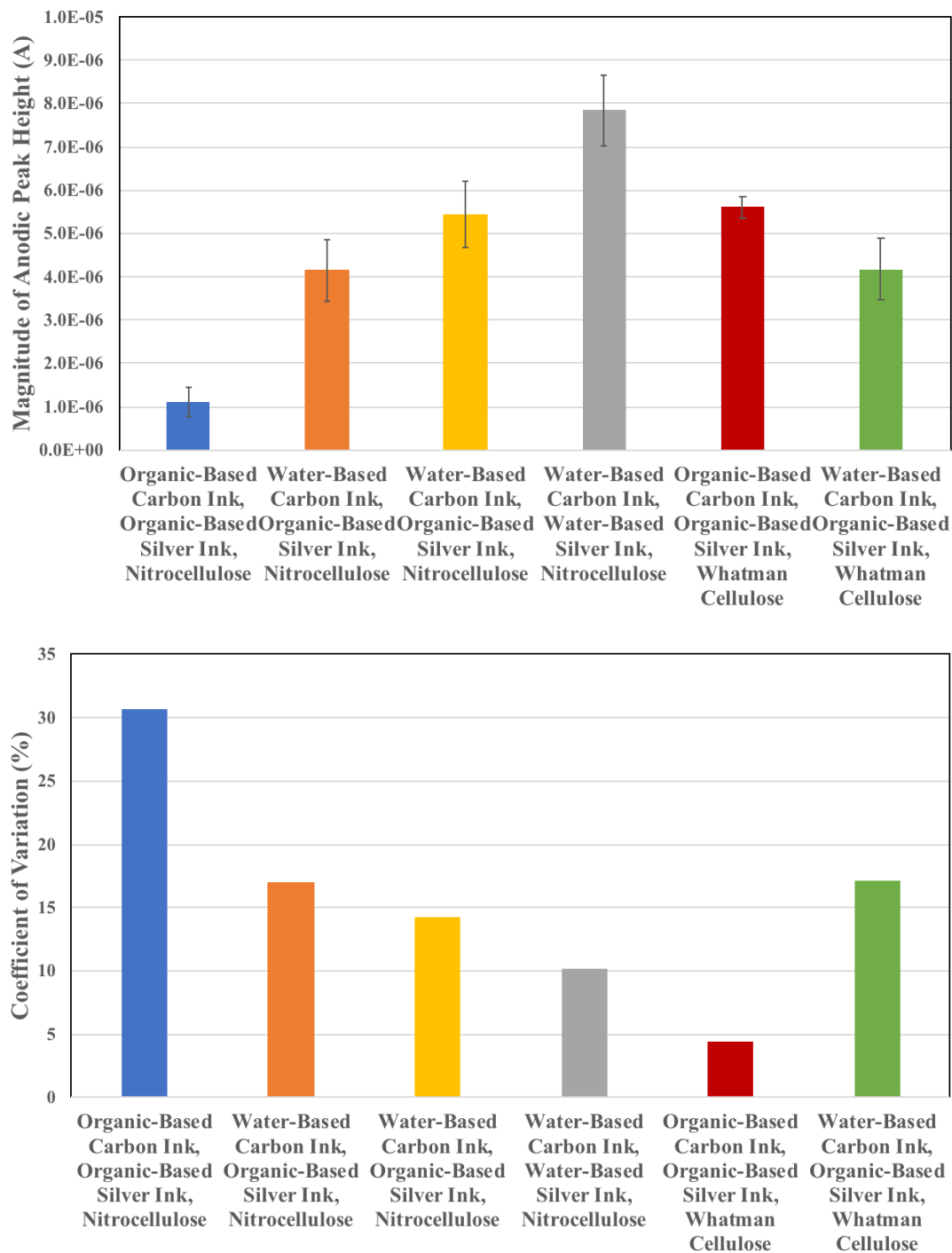


Figure 19: Overall results from the Material Compatibility study that compared two substrates, two carbon ink solvents, and two silver ink solvents. The most optimal combination determined utilized the Whatman cellulose substrate, the organic-based carbon ink, and the organic-based silver reference ink.

Following the three studies, it was determined that the nitrocellulose substrate was too sensitive for the electrode system as shown through the high coefficients of variation and the degradation of the substrate around the area of the electrodes.

The most optimal combination utilized the Whatman cellulose substrate, the organic-based solvent carbon ink, and the organic-based solvent silver reference ink. This combination produced the second highest magnitude of the average anodic peak height with the smallest coefficient of variation. The combination of the organic-based inks on the Whatman cellulose was utilized for further testing discussed in the next chapter.

Chapter Three – Shelf Life Study

Introduction

One issue that arises when utilizing diagnostic devices is their shelf life. The shelf life of a diagnostic device is the amount of time that a device can go unused following fabrication, and still yield predictable behavior when finally used. The purpose of this study was to determine the effect that storage time would have on the screen-printed electrode system. This would help to determine if the screen-printed carbon electrode devices were a viable alternative to the commercially available diagnostic devices.

The study utilized the most optimal pairing determined in the previous chapter. These devices were fabricated on Whatman cellulose with the organic-based solvent carbon ink, and the organic-based solvent silver ink. This card combination produced the second highest magnitude of the average anodic peak height with the smallest coefficient of variation making it the most reliable combination to be used in the devices.

Electrodes were screen printed within the same fabrication set and tested on various days after the initial fabrication to determine how the signal changes as a function of storage time. Tests were conducted on the same day as fabrication (Day 0), the day after (Day 1), three days after (Day 3), seven days after (Day 7), fourteen days after (Day 14), and twenty-eight days (Day 28) after initial fabrication of the devices.

Devices were compared based on the magnitude of the average anodic peak heights and their coefficient of variation. A high magnitude of the average anodic peak height was desired as it correlates to signal and a low coefficient of variation was desired as it represents the reproducibility of the devices.

Methods and Materials

Materials and Inks Used

This study used an organic-based solvent carbon ink and an organic-based solvent silver ink (Gwent). The substrate was Whatman cellulose (EMD Millipore). Ferrocenemethanol (EMD Chemicals) was the electrolyte solution used. The commercial three electrode system (CHI Instruments) was used for comparison.

Fabrication for the devices included 10-mil Mylar backing (Tekra), 1-mil Mylar screens (Tekra), and a squeegee. Devices were designed with Draftsight (Dassault Systems) and materials were cut with a CO₂ laser (Universal). A wax printer (Xerox ColorCube) and an oven (Thermo) were utilized for defining a well area. CV scans were performed using a potentiostat and macro functions (CHI Instruments).

Cyclic Voltammetry Testing

The signal was read from the potentiostat and saved as a file within the Electrochemical software. The files were analyzed using a custom MATLAB (Natick) program that exported an Excel (Microsoft) file. All peak heights were determined through the CHI software. The values were graphed and compared based on the magnitude of the anodic peak heights and the coefficient of variation.

Card Fabrication

A substrate holder was cut using the laser printer and 10-mil adhesive Mylar sheets to hold the Whatman devices in place during the screen-printing process. A silver stencil and a carbon stencil were cut using the laser printer and 1-mil Mylar. Whatman cards were cut in the laser printer and the well area was printed utilizing the wax printer. The cards were baked at 100°C in the oven for five minutes following the wax printing. The silver stencil was taped on top of the substrate holder with a Whatman card inside. The organic-based silver reference ink was mixed and placed at the top of the design on the silver stencil and a squeegee was pulled down the length of the Mylar stencil with constant pressure to imprint the silver design onto the substrate. The card was then baked at 100°C for ten minutes. After removing the silver stencil, the carbon stencil was taped on top of the substrate holder. The organic-based carbon ink was mixed and placed at the top of the carbon design and pulled down with a squeegee to imprint the carbon design onto the substrate. The cards were then placed in the oven at 100°C for ten minutes. After the baking period, the cards were cut into six individual devices which were then ready for testing. An example of the card layouts can be seen in Figure 20.

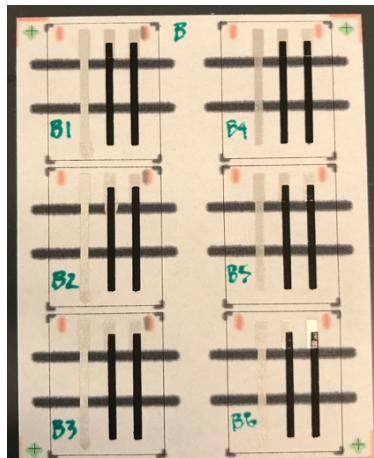


Figure 20: Top view of card B. Each card contains six devices. Four total cards were fabricated during this study (A-D). Devices are created on card for efficiency and consistency during the screen-printing process.

Detection Methods

Screen-printed Carbon Electrodes

Devices were placed on a stand with a Mylar holder and secured using an alligator clip. The three electrodes were placed on their designated connections as seen in Figure 21. The white electrode clipped to the reference electrode, the red electrode clipped to the counter electrode, and the green electrode clipped to the working electrode.

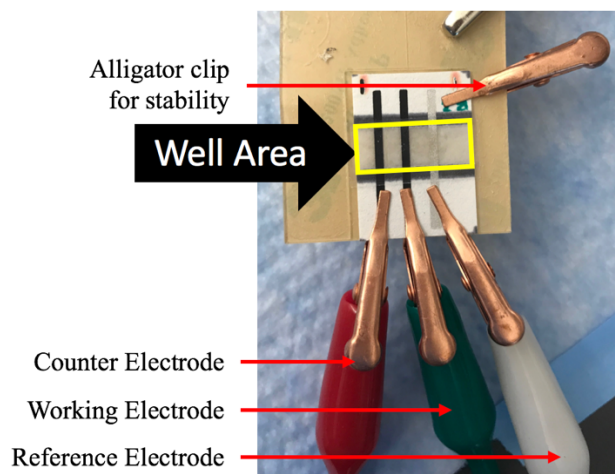


Figure 21: A single electrochemical sensing device interfacing with CHI potentiostat. The well is defined by wax boundaries (black ink) with electrodes spanning the fluid well.

The Electrochem software was opened and the scan rate and applied voltage were set. For the devices, 13.5 μL of 2.0 mM FCM was pipetted into the well space as the electrolyte solution. This volume was 100% of the capacity of the well area. Testing began one minute after adding the FCM solution, allowing the surface to fully wet out. After testing completes the specified number of scans, the devices were disconnected, and the data was imported to MATLAB.

Commercially Available Electrodes

Electrodes were kept in their own containers to protect their surfaces. Each electrode was removed from the containers and placed with the tip into the electrolyte solution. The three electrode connections were placed on their designated connection (Fig. 22). The white electrode clipped to the reference electrode, the red electrode clipped to the counter electrode, and the green electrode clipped to the working electrode. Each electrode was observed for bubbles on the surface or for contacting clips as both of these instances could lead to faulty data.

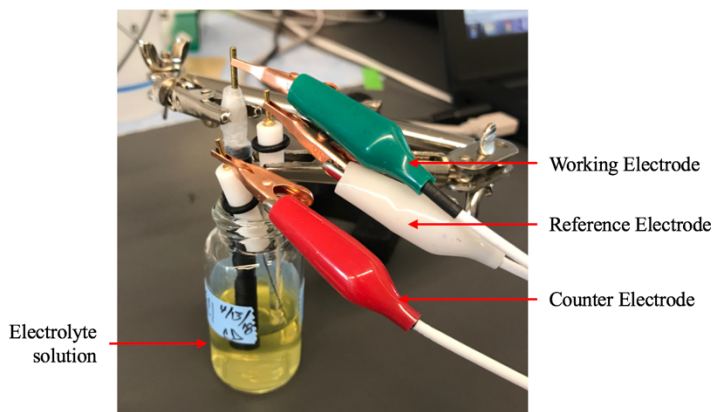


Figure 22: The connections from the potentiostat to the commercial electrode system. Each electrode is placed into the formulated FCM solution ensuring there are no air bubbles on the surface of any of the electrodes.

Results and Discussion

Commercial Electrode System

After the 28-day testing period, the commercial electrode system showed no decrease in signal strength when it was placed into the electrolyte solution (Fig. 23). This proved

that if decrease in signal strength occurred in the screen-printed devices, it would be a result of the cards and not the electrolyte solution.

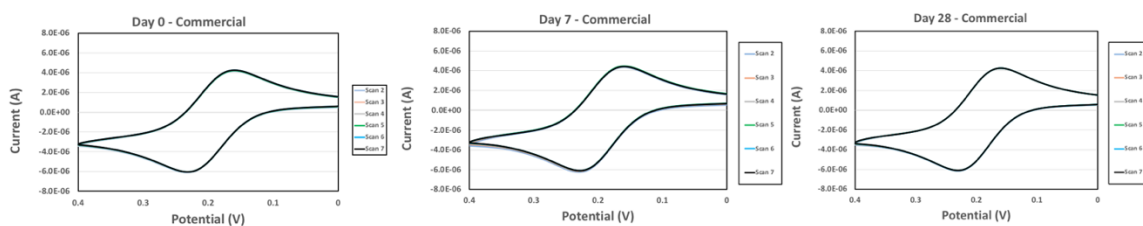


Figure 23: Control for the FCM electrolyte solution utilizing the commercially available electrodes. Testing showed no decreased in signal strength when utilizing the commercial system over the 28-day period.

Day Zero and Day One

All devices were fabricated concurrently to show that variations between cards were effects of the storage time. The initial day of fabrication was denoted as Day Zero for analysis. All devices from Day Zero (N=4) and Day One (N=4) showed consistent wetting, low coefficients of variations, and consistent the anodic peak heights (Fig. 24). All device scans can be seen in Appendix 4.

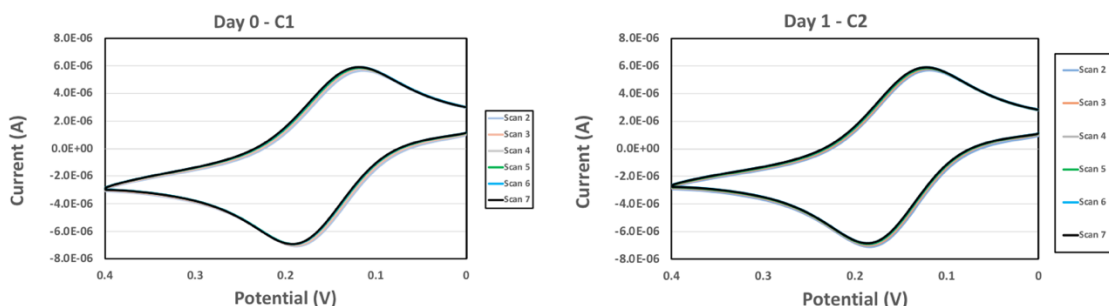


Figure 24: Cyclic voltammetry scans of individual devices that were fabricated on the same card but were analyzed on Day Zero and Day One. Both devices presented consistent anodic peak heights and a low coefficient of variation.

Day Three and Day Seven

The devices from Day Three did not show consistent wetting throughout testing. Device C3 had difficulty wetting out and therefore produced inconsistent results (Fig 25). In addition, device B3 produced inconclusive scans. This device was omitted from the Day Three data analysis. Because there was no preliminary data on what the shelf

life of the devices may be, earlier testing days were prioritized. Therefore, in order to maintain testing four devices each testing day, device A4 was tested on Day Three.

The devices from Day Seven showed consistent wetting through the well area throughout testing. Device A5 was tested with this set in order to maintain the number of devices tested.

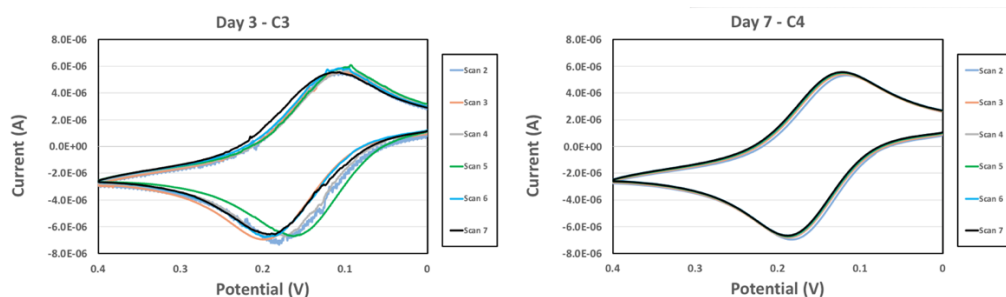


Figure 25: Cyclic voltammetry scans of individual devices that were fabricated on the same card but were analyzed on different days. Issues with device C3 lead to higher coefficient of variation however both devices presented consistent anodic peak heights.

Day Fourteen and Day Twenty-Eight

The devices from Day Fourteen and Day Twenty-eight showed consistent wetting through the well area throughout testing. There were errors on devices B5, D5, B6, and D6 so this data was not included in the analysis. Errors are further detailed in Appendix 4. The scans for device C5 were overridden by the scans for D5 so the cycle was run an additional time with water rather than the electrode solution. This produced smaller anodic and cathodic peak heights and were omitted from analysis (Fig. 26).

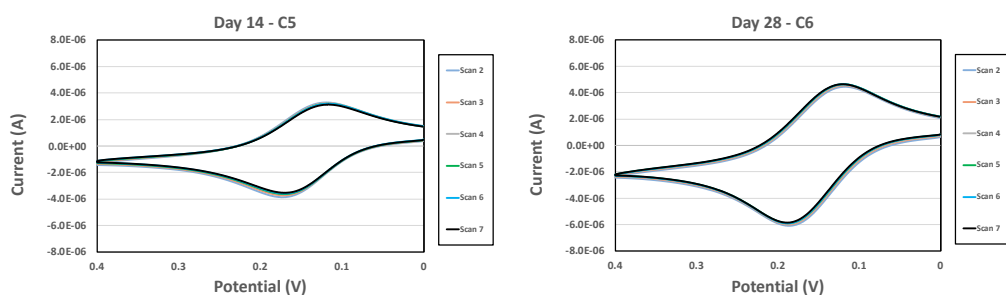


Figure 26: Cyclic voltammetry scans of devices C5 and C6 tested fourteen and twenty-eight days after initial fabrication respectively. Scans for device C5 was overridden by the scans for D5 and was omitted from analysis.

Conclusion

Overall results comparing all devices on all testing days from the Shelf Life study can be viewed in Figure 27, Figure 28 and in Table 3.

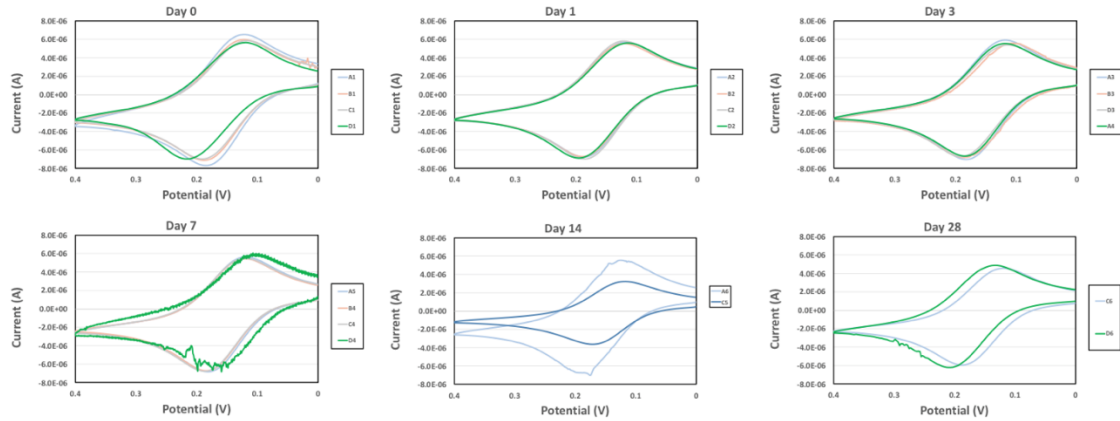


Figure 27: Cyclic voltammety scans for the comparison of all usable devices from all days of testing for the Shelf Life study.

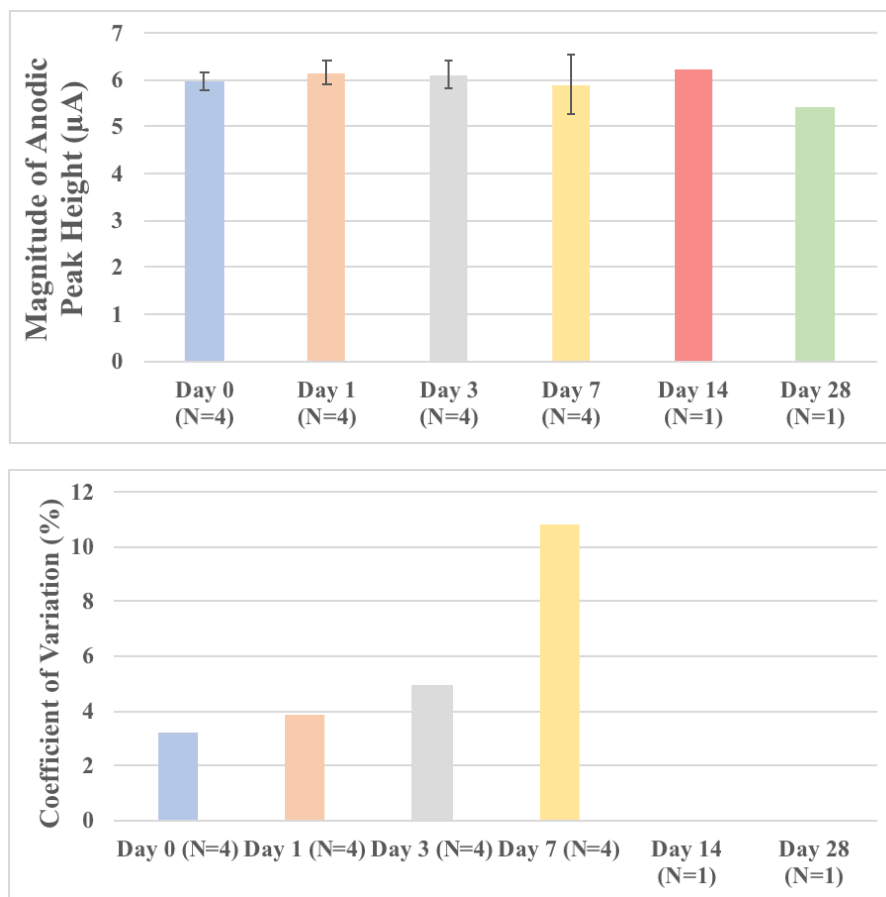


Figure 28: Comparison of all devices on each day across the twenty-eight day shelf life study.

Table 3: Magnitude of the average anodic peak heights and coefficient of variation for the comparison of all cards from all days of testing for the Shelf Life study.

Day	0	1	3	7	14	28
No. of Cards Tested	4	4	4	4	1	1
Average Magnitude of Anodic Peak Height (μA)	6.16	5.97	6.12	5.89	6.23	5.43
Coefficient of Variation (%)	3.85	3.23	4.97	10.8	N/A	N/A

Following these results, the data supports that the shelf life of the organic-based solvent carbon and silver inks on Whatman cellulose devices is seven days after initial fabrication. A t-test was performed showing that there is no significant difference between the number of days after the cards were fabricated and the magnitude of the anodic peak height. Even though there was no significant change in the signal across days, due to the limited number of replications on the later days, this study supports a shelf life of seven days.

Chapter 4 – Conclusions and Next Steps

Summary of Conclusions

The previous chapters evaluated the signals produced from two carbon inks, two silver inks, and two substrates in an electrode system and determined their viability as an alternative to lab-based testing. Devices were observed for their signal and reproducibility.

Chapter Two compared the various combinations of the solvents in the carbon ink and the silver ink on two substrates. Both the carbon and the silver inks contained either an organic-based or a water-based solvent. The two substrates were nitrocellulose and Whatman cellulose. Three total studies were conducted to compare the various pairings.

The first study compared the organic-based and water-based carbon inks on nitrocellulose with the organic-based silver ink. This study found that the water-based carbon ink produced a higher magnitude average anodic peak ($4.15\mu\text{A}$) with a lower coefficient of variation (17.0 %).

The next study compared the organic-based and water-based silver inks on nitrocellulose with the water-based carbon ink. This study found that the water-based carbon ink produced higher magnitude average anodic peaks ($7.84\mu\text{A}$) with a lower coefficient of variation (10.2 %).

The final study compared the organic-based and water-based carbon inks on Whatman cellulose with the organic-based silver ink. This study found that the organic-based carbon ink produced higher magnitude average anodic peaks ($5.61\mu\text{A}$) with a lower coefficient of variation (4.47 %).

Issues with the ink penetration onto the delicate nitrocellulose device caused issues with the reproducibility for the devices and lead to high coefficients of variation. It was determined that the most optimal combination was the Whatman cellulose substrate, the organic-based carbon ink, and the organic-based silver ink. This combination produced the second highest magnitude average anodic peak height with the smallest coefficient of variation and was used in the shelf life study.

Chapter Three determined the effect that storage time has on the screen-printed devices. All devices were fabricated on Day Zero and were tested on pre-determined periods of time after initial fabrication. These periods were determined to be Day Zero, Day One, Day Three, Day Seven, Day Fourteen, and Day Twenty-eight. The early testing days were prioritized for data points as we were most concerned that the devices had a shelf life that was less than Seven days. A commercial electrode system was utilized each testing day to determine if there was a difference in the FCM electrolyte solution within the month-long testing period.

There was not a statistically significant difference between the number of days after the cards were tested and the magnitude of the average anodic peak heights. This shows that the signals were just as sensitive on Day Twenty-eight as they were on the initial fabrication day. Even though there was no significant change in the signal across days, due to the limited number of replications on the later days, this study supports a shelf life of seven days.

Next Steps

Extending Shelf Life Study

A t-test showed that through twenty-eight days of testing, there was no statistical significance between the magnitude of the anodic peak height and the number of days after fabrication. This statement has less of an impact because of the reduced number of devices that were useable after Day Seven. An additional shelf life study should be conducted that prioritizes the later time points in order to determine the true shelf life of the devices. More time points should be added to the shelf life study as well as fabricating more cards that could be utilized during these days as backups. Extending the shelf life study to Day 48 and Day 60 testing could help to determine if the devices could be used up to two months after fabrication.

More Robust Screen-Printing Process

The current method for the fabrication of the devices should be optimized and standardized. Throughout both studies, issues were observed with the thickness and the distribution of both the silver and carbon inks. Because these cards are fabricated by hand, there is a large potential for human error and variability between cards. An issue was observed with the entire B card during the shelf life study that resulted in many of these devices being labeled as unusable. Developing a more robust process or fabrication process will only decrease the coefficient of variation further providing more reproducible devices.

Development of a Compact Potentiostat and Cyclic Voltammetry System

The main purpose of both studies was to develop an electrochemically sensing electrode system that could be combined with a paper-based microfluidic device. This is a beneficial system because it provides an alternative to performing laboratory-based assays in low resource settings (Yetisen, 2013). This thesis attempted to optimize the paper-based aspect of this system by providing an optimal combination of the inks and substrate used. In order to advance this project further, the potentiostat and the testing system would need to become more compact and user-friendly for use in low resource settings. Currently, the potentiostat requires the user to set up the Electrochem software with the correct voltage and scan rates, clip the electrode connections to the appropriate

electrode, and to analyze the results using three different computer programs. This process requires electricity and training of the individual. In addition, the entire potentiostat is a large, bench-top device that is impractical for remote usage. This equipment would need to include the entire potentiostat function as well as contain the electrode clips in order to have the reaction readout occur within the potentiostat. Then the data from the equipment would need to either be transferred to an external device (such as a cell phone) or displayed directly onto a readout screen. The development of this equipment would be the next steps to creating an entire system that is compact, user-friendly, and an accurate alternative to laboratory-based diagnostics.

Appendix 1 – Organic-Based Conductive Carbon Ink with Organic-Based Silver Reference Ink on Nitrocellulose (Results from 1/16/18)

Table 1-1: Average anodic peak values and coefficients of variation for each device. These averages are taken from six of the seven scans that were completed during the testing period.

Organic-Based Carbon Ink with Organic-Based Silver Ink on Nitrocellulose							
Card Number	A11	A12	A13	A21	A22	A23	Average of All Devices
Magnitude of the Anodic Peak Height (μA)	1.49	1.03	0.60	1.49	0.98	1.04	1.11
Coefficient of Variation (%)	13.8	4.22	35.9	26.1	14.51	4.94	30.6
Water-Based Carbon Ink with Organic-Based Silver Ink on Nitrocellulose							
Card Number	B11	B12	B13	B21	B22	B23	Average of All Devices
Magnitude of the Anodic Peak Height (μA)	4.16	N/A	4.56	4.46	4.65	2.93	4.15
Coefficient of Variation (%)	4.77	N/A	1.97	2.70	0.96	24.7	17.0

Appendix 1 – Organic-Based Conductive Carbon Ink with Organic-Based Silver Reference Ink on Nitrocellulose (1/16/18)

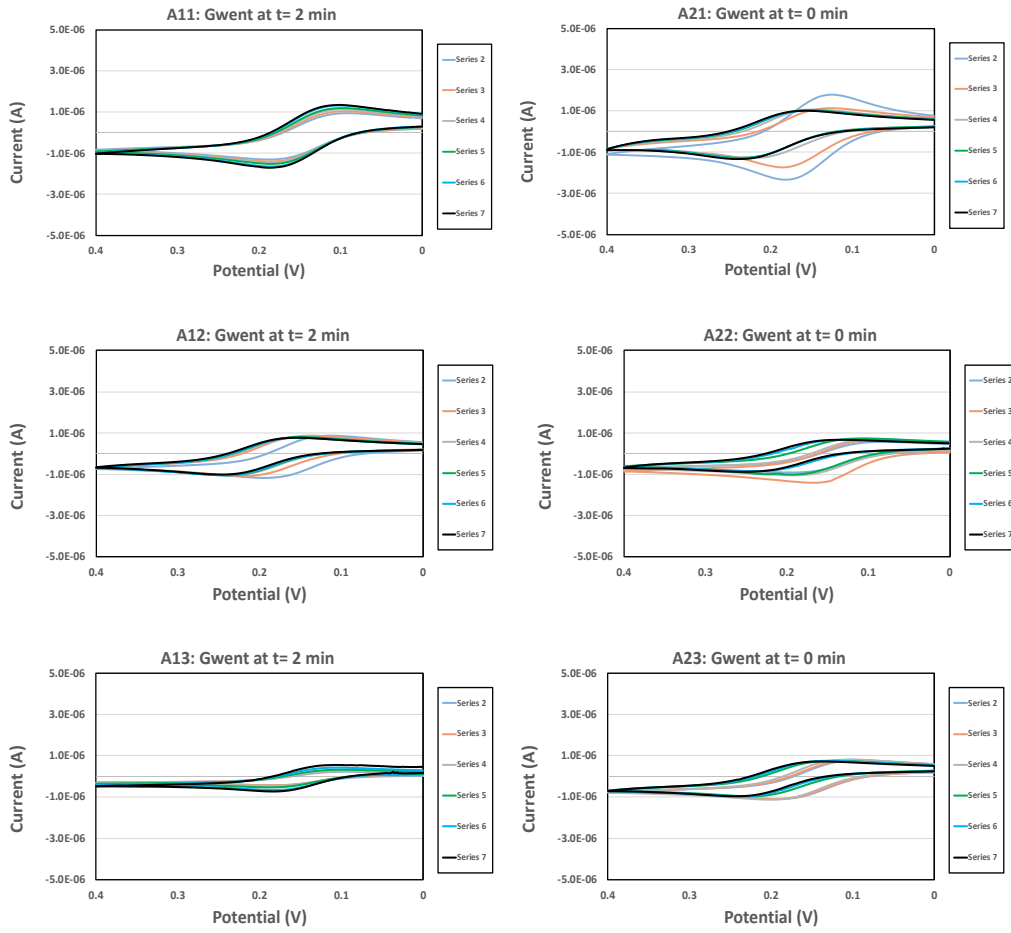


Figure 1-1: Individual device data from first set of devices. These cards contained organic-based carbon ink and organic-based silver ink on nitrocellulose.

Appendix 1 –Water-Based Conductive Carbon Ink with Organic-Based Silver Reference Ink on Nitrocellulose (1/16/18)

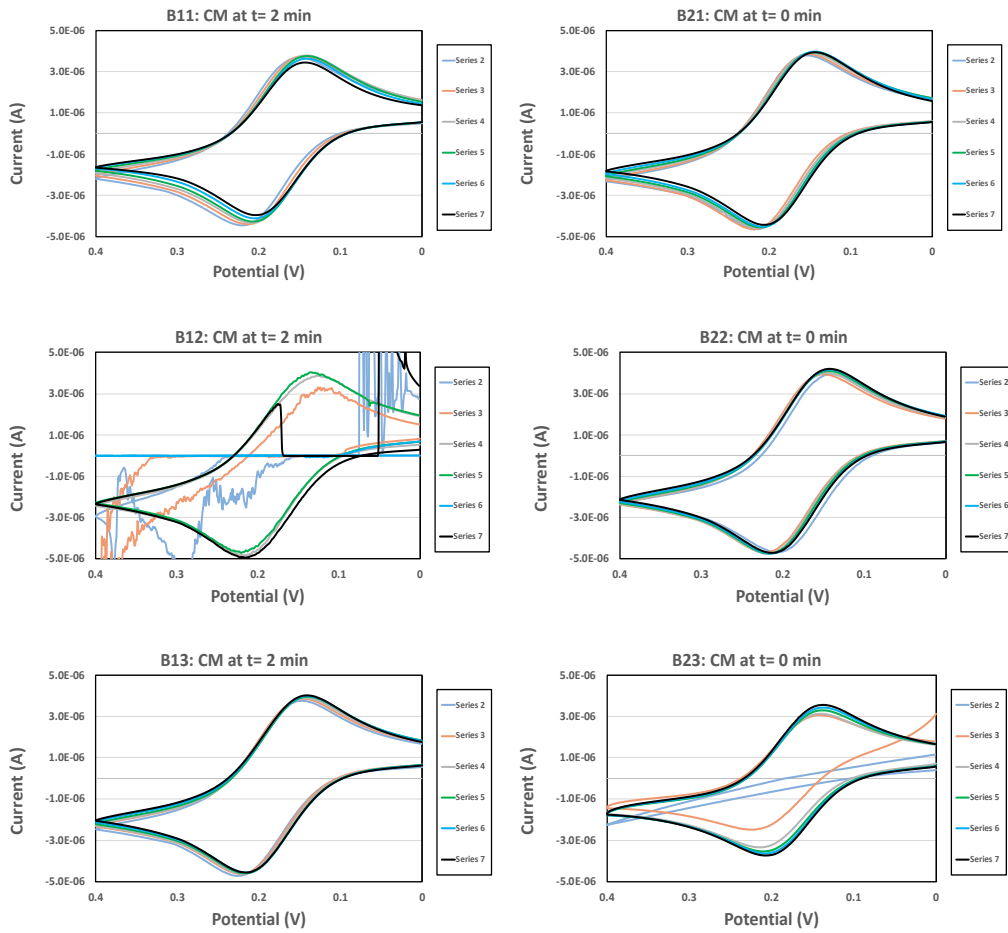


Figure 1-2: Individual device data from first set of devices. These cards contained water-based conductive carbon ink and organic-based silver reference ink on nitrocellulose. Card B12 was removed from analysis.

Appendix 2 – Organic-Based vs. Water-Based Silver Reference Ink with Water-Based Conductive Carbon Ink on Nitrocellulose (Results from 2/28/18)

Table 2-1: Average anodic peak values and the coefficient of variations for each nitrocellulose device. These averages are taken from last six of the seven scans that were completed during the testing period.

Organic-Based Silver Ink with Water-Based Carbon Ink on Nitrocellulose			
Card Number	1	2	Average of All Devices
Magnitude of the Anodic Peak Height (μA)	5.07	5.81	5.44
Coefficient of Variation (%)	18.0	6.89	14.2
Water-Based Silver Ink with Water-Based Carbon Ink on Nitrocellulose			
Card Number	1	2	Average of All Devices
Magnitude of the Anodic Peak Height (μA)	7.67	8.01	7.84
Coefficient of Variation (%)	9.56	11.2	10.4

Appendix 2 – Organic-Based vs. Water-Based Silver Reference Ink with Water-Based Conductive Carbon Ink on Nitrocellulose (Results from 2/28/18)

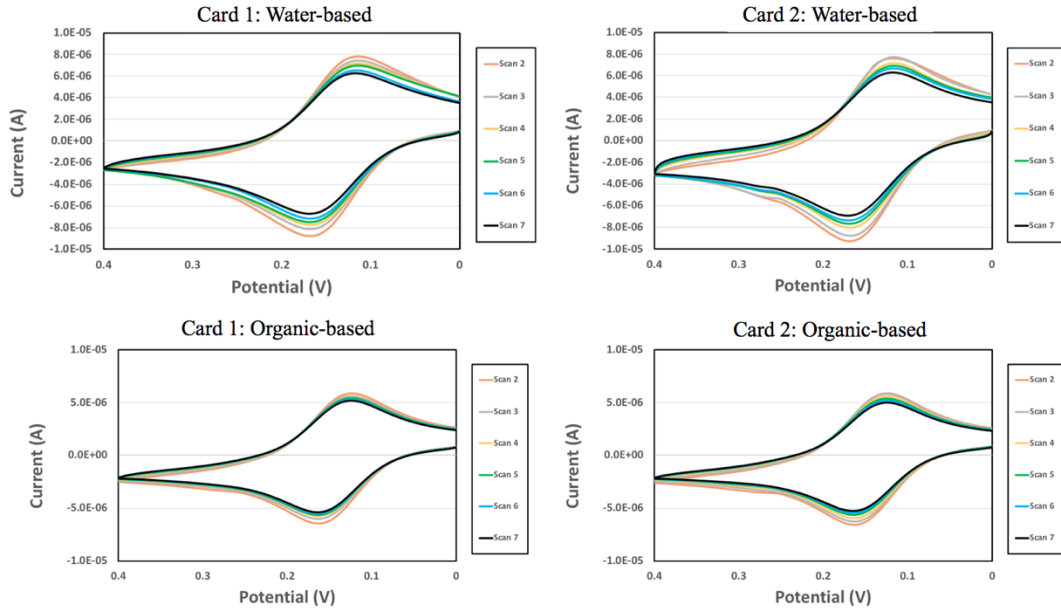


Figure 2-1: Individual card results comparing the organic-based and water-based silver reference inks on a nitrocellulose substrate.

Appendix 3 – Organic-Based vs. Water-Based Conductive Carbon Ink with Organic-Based Silver Reference Ink on Whatman Cellulose (Results from 1/23/18)

Table 3-1: Average anodic peak values and coefficients of variation for each device. These averages are taken from last six of the seven scans that were completed during the testing period.

Organic-Based Carbon Ink with Organic-Based Silver Ink on Whatman Cellulose				
Card Number	1	2	3	Average of All Devices
Magnitude of the Anodic Peak Height (μA)	5.75	5.75	5.32	5.61
Coefficient of Variation (%)	5.38	7.48	0.849	4.47
Water-Based Carbon Ink with Organic-Based Silver Ink on Whatman Cellulose				
Card Number	1	2	3	Average of All Devices
Magnitude of the Anodic Peak Height (μA)	3.65	4.98	3.86	4.16
Coefficient of Variation (%)	10.9	14.6	12.3	17.1

Appendix 3 – Organic-Based vs. Water-Based Conductive Carbon Ink with Organic-Based Silver Reference Ink on Whatman Cellulose (Results from 1/23/18)

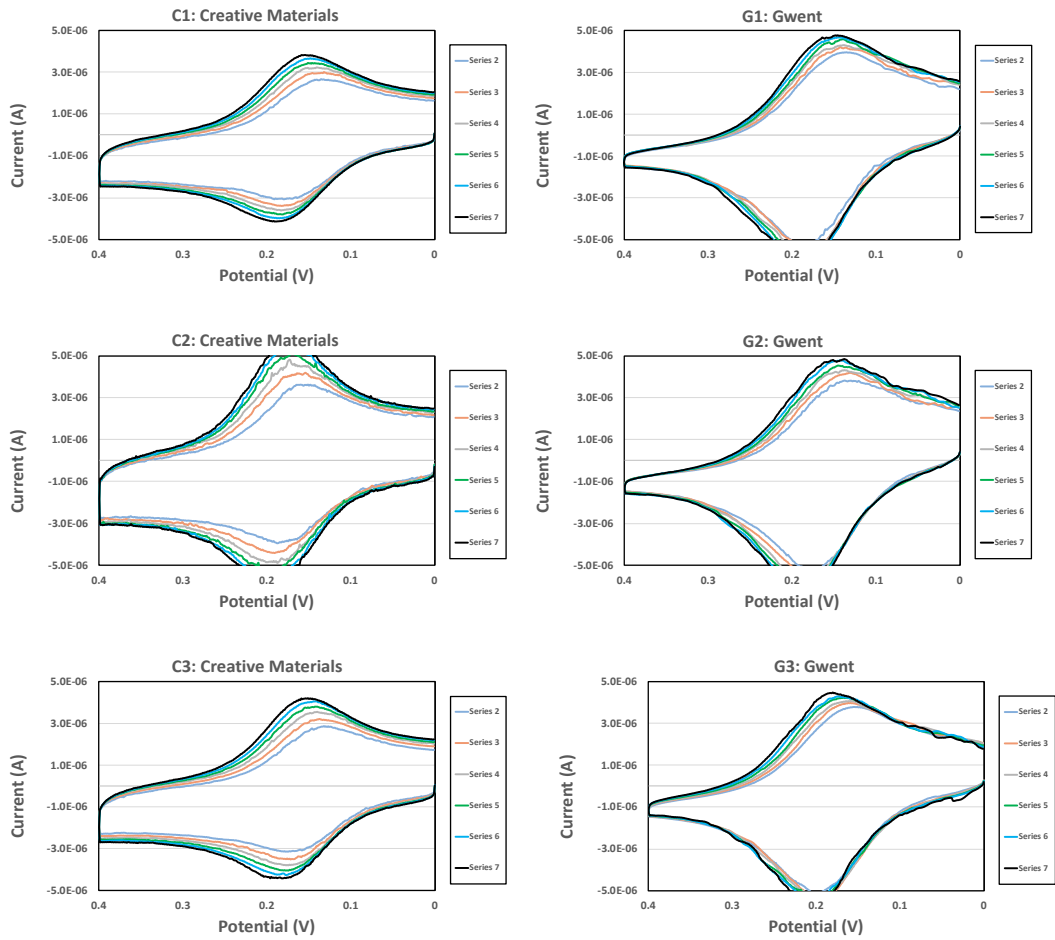


Figure 3-1: Individual device data from second set of devices. These devices compared organic-based conductive carbon ink and organic-based conductive carbon ink with organic-base silver reference ink on Whatman cellulose.

Appendix 4 – Shelf Life Study

Day Zero

Table 4-1: Anodic peak values and the coefficient of variations for each device on Day Zero and Day One. The averages are taken from the final six of the seven total scans that were completed during the testing period.

Day Zero					
Device Number	A1	B1	C1	D1	Average of All Devices
Peak Value (μA)	-6.21	-6.11	-5.89	-6.44	-6.16
Coefficient of Variation (%)	2.09	1.68	2.11	2.37	3.85
Day One					
Device Number	A2	B2	C2	D2	Average of All Devices
Peak Value (μA)	-5.79	-5.90	-6.09	-6.10	-5.97
Coefficient of Variation (%)	1.89	1.48	1.48	4.05	3.23

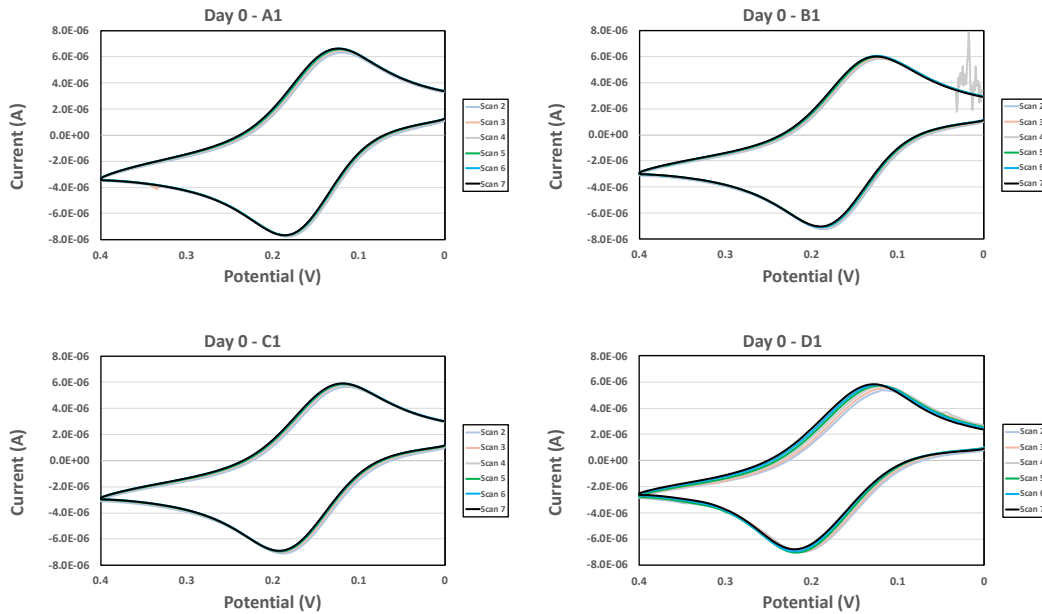


Figure 4-1: Individual device data from devices tested on the initial day of fabrication (Day Zero). Four total devices were tested and analyzed this day.

Appendix 4 – Shelf Life Study

Day One:

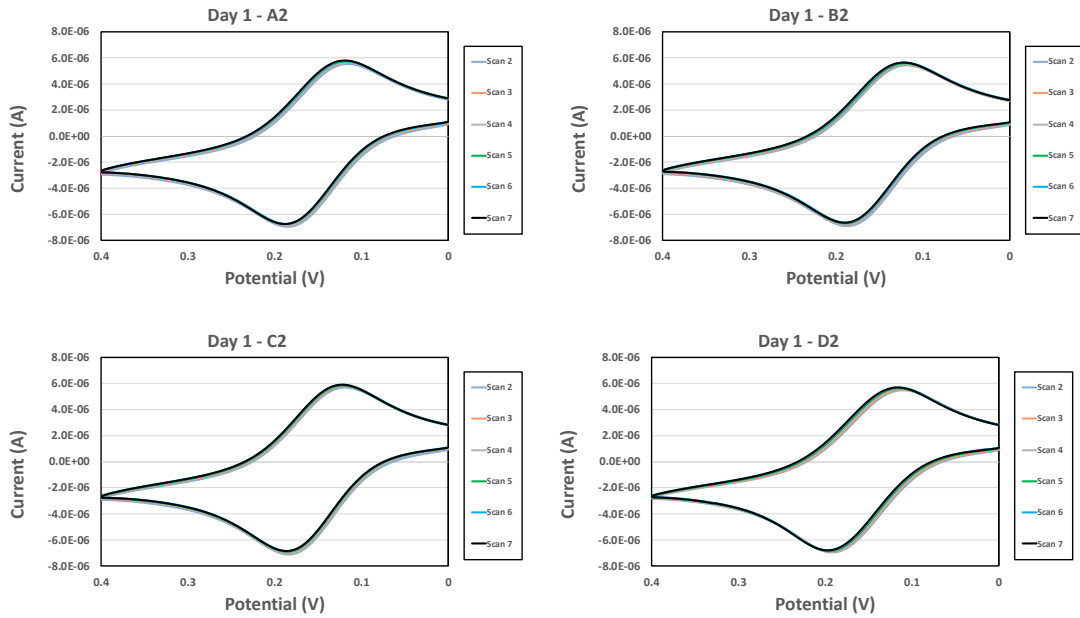


Figure 4-2: Individual device data from devices tested on the day after fabrication (Day One). Four total devices were tested and analyzed this day.

Table 4-2: Anodic peak values and the coefficient of variations for each device on Day Three and Day Seven. The averages are taken from the final six of the seven total scans that were completed during the testing period.

Day Three						
Card Number	A3	B3	C3	D3	A4	Average
Peak Value (μA)	-6.32	N/A	-6.13	-6.07	5.95	-6.12
Coefficient of Variation (%)	5.42	N/A	7.08	2.01	2.16	4.97
Day Seven						
Card Number	A5	B4	C4	D4	Average	
Peak Value (μA)	-6.13	-6.16	-6.05	-4.59	-5.89	
Coefficient of Variation (%)	3.45	1.55	0.84	21.0	10.8	

Appendix 4 – Shelf Life Study

Day Three:

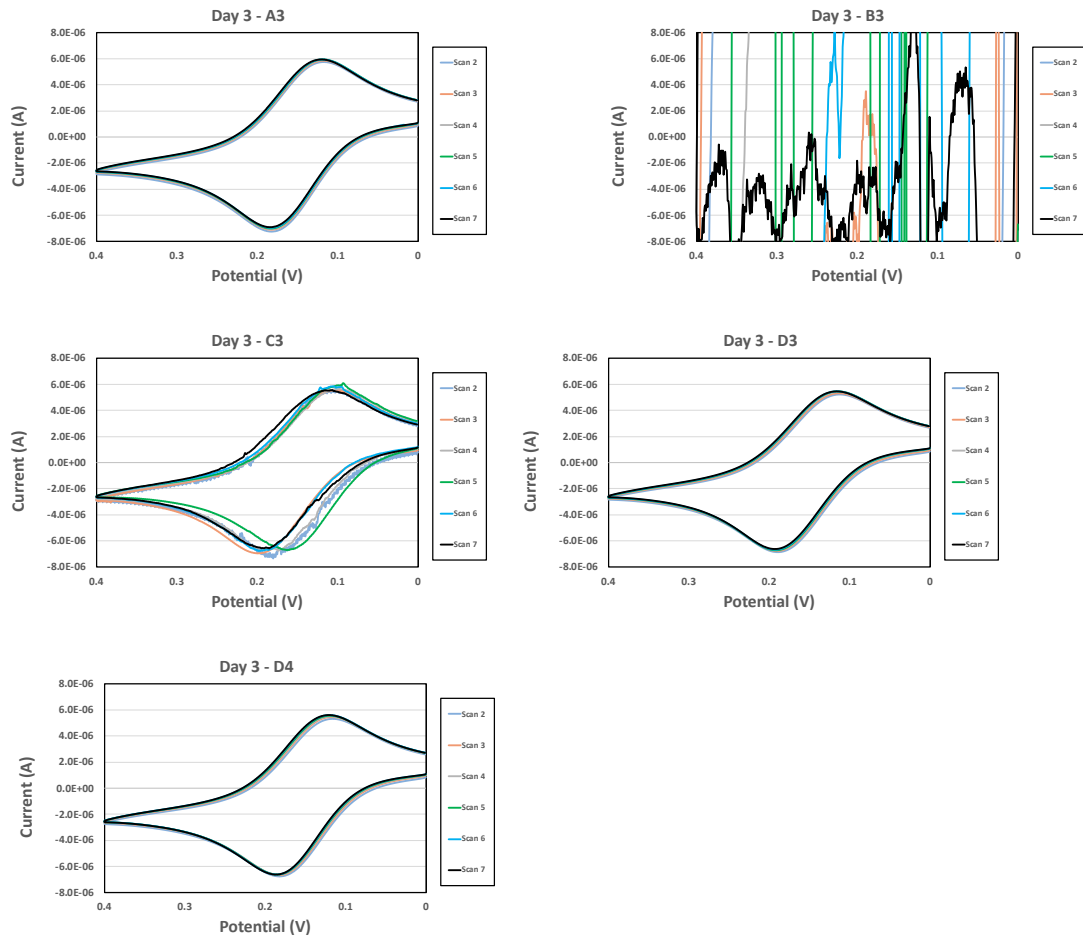


Figure 4-3: Individual device data from devices tested three days after fabrication (Day Three). Five total devices were tested and four were analyzed this day.

Appendix 4 – Shelf Life Study

Day Seven:

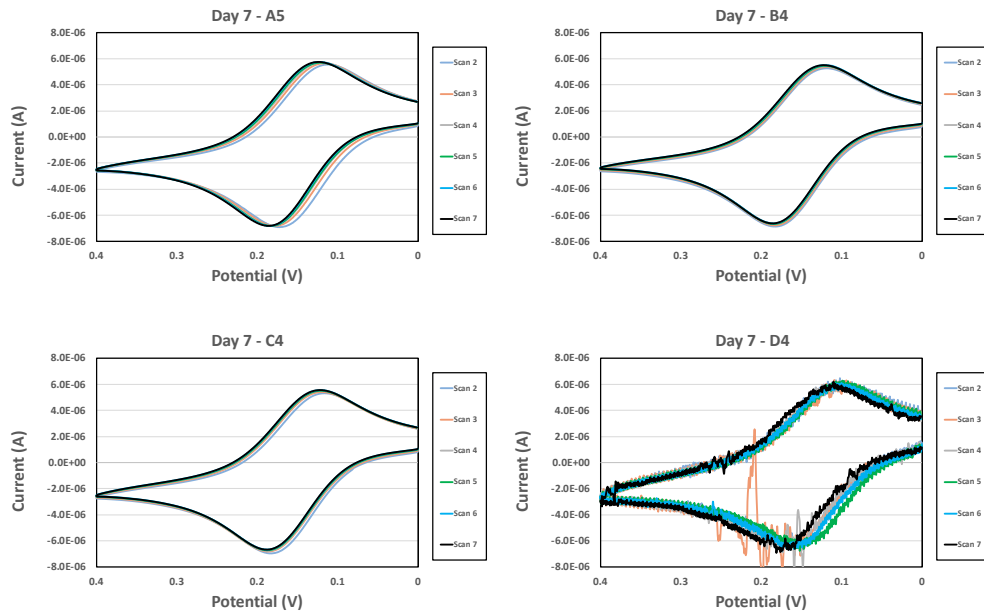


Figure 4-4: Individual device data from devices tested seven days after fabrication (Day Seven). Four total devices were tested and analyzed this day.

Appendix 4 – Shelf Life Study

Table 4-3: Anodic peak values and the coefficient of variations for each device on Day 14 and Day 28. The averages are taken from the final six of the seven total scans that were completed during the testing period.

Day Fourteen					
Card Number	A6	B5	C5	D5	Average
Peak Value (μA)	-6.82	N/A	-3.07	N/A	-4.93
Coefficient of Variation (%)	21.1	N/A	2.40	N/A	44.2
Day Twenty - Eight					
Card Number	B6	C6	D6	Average	
Peak Value (μA)	N/A	-5.43	N/A	-5.43	
Coefficient of Variation (%)	N/A	1.82	N/A	1.82	

Day Fourteen:

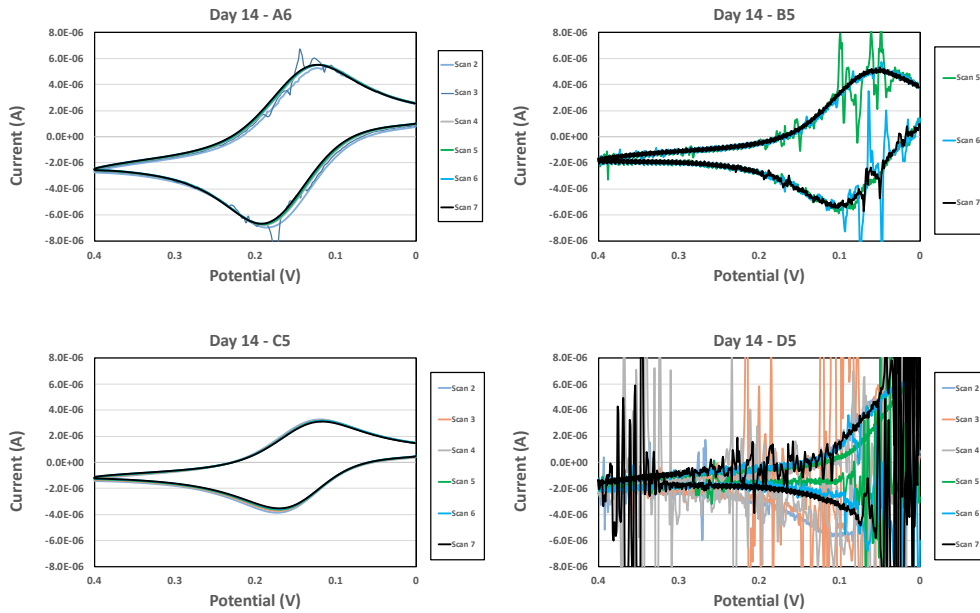


Figure 4-5: Individual device data from devices tested fourteen days after fabrication (Day Fourteen). Four total devices were tested and two were analyzed this day.

Appendix 4 – Shelf Life Study

On Day Fourteen, device B5 resulted in inconclusive scans as a shift in the peaks after the fourth scan showed an issue with the reference ink. After observations of the surface of the card, an even layer of silver was not printed onto the device (Fig. 4-6) resulting in poor scans for various B devices (Fig. 4-7). Card B experienced many issues with the silver ink on the reference electrodes seen on Day 7, 14, and 28 devices. Because this issue was not seen on other cards, this is most likely attributed to the fabrication of the devices and the use of the 1-mil Mylar silver reference ink stencil.

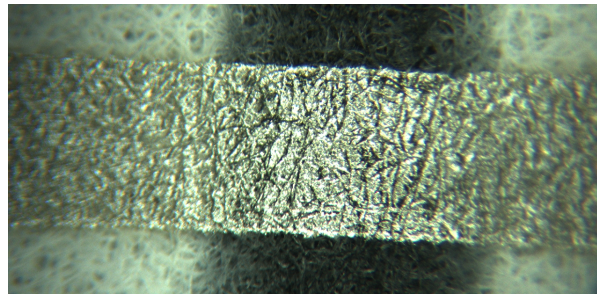


Figure 4-6: Uneven reference ink on a reference electrode from card B devices. This uneven application of the reference ink lead to inconclusive scans.

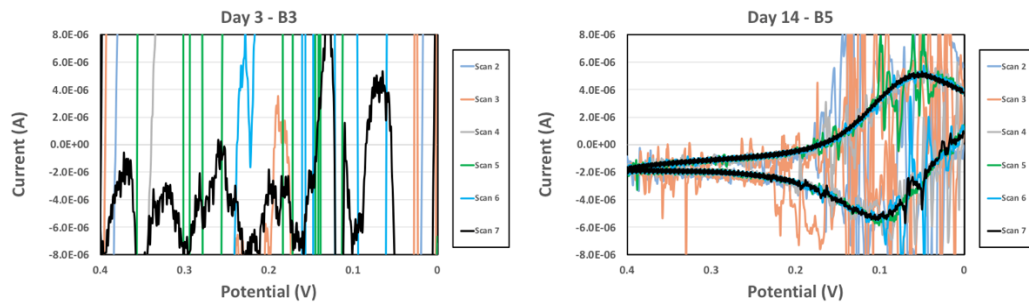


Figure 4-7: Devices B3 and B5 both had issues establishing a reference from the reference electrodes. This is attributed to issues in the screen-printing fabrication process with the 1-mil Mylar stencils.

Day Twenty-Eight:

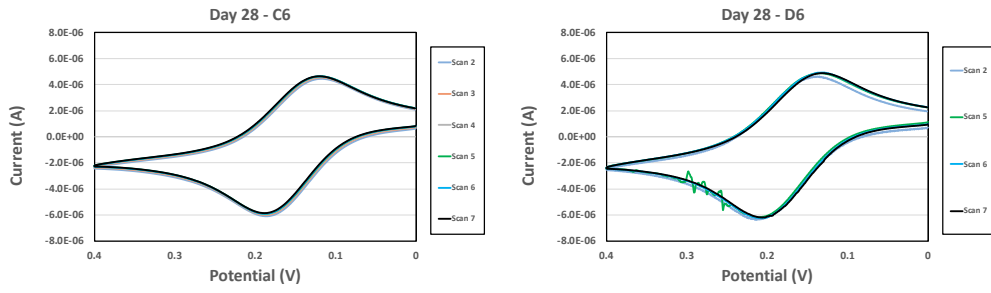


Figure 4-8: Individual device data from devices tested twenty-eight days after fabrication (Day Twnty-Eight). Three total devices were tested and only one was analyzed this day.

References

Aljabali, A. A., Barclay, J. E., Butt, J. N., Lomonossoff, G. P., & Evans, D. J. (2010). Redox-active ferrocene-modified Cowpea mosaic virus nanoparticles. *Dalton transactions*, 39(32), 7569-7574.

Bacher, A. (2003, February 4). Electrochemical cell and electrodes for cyclic voltammetry. Retrieved from <http://www.chem.ucla.edu/~bacher/CHEM174/equipment/CV1.html>.

Betancur, V., Sun, J., Wu, N., & Liu, Y. (2017). Integrated lateral flow device for flow control with blood separation and biosensing. *Micromachines*, 8(12), 367.

Cheng, C. M., Kuan, C. M., & Chen, C. F. (2015). *In-vitro diagnostic devices: introduction to current point-of-care diagnostic devices*. Springer.

Devengenzo, M. (2019). Standard Electrodes. Retrieved from [https://chem.libretexts.org/Bookshelves/Analytical_Chemistry/Supplemental_Modules_\(Analytical_Chemistry\)/Electrochemistry/Electrodes/Standard_Hydrogen_Electrode](https://chem.libretexts.org/Bookshelves/Analytical_Chemistry/Supplemental_Modules_(Analytical_Chemistry)/Electrochemistry/Electrodes/Standard_Hydrogen_Electrode).

Dimitrov, D. I., et al. *Capillary Rise in Nanopores: Molecular Dynamics Evidence for the Lucas-Washburn Equation*. Institute for Chemical Physics, Bulgarian Academy of Sciences, 30 Mar. 2007.

Downs, C., Nejely, A., & Fu, E. (2018). Disposable fabric-based electrochemical sensors fabricated from wax-transfer-printed fluidic cells and stencil-printed electrodes. *Analytical methods*, 10(29), 3696-3703.

Elgrishi, N., Rountree, K. J., McCarthy, B. D., Rountree, E. S., Eisenhart, T. T., & Dempsey, J. L. (2017). A practical beginner's guide to cyclic voltammetry. *Journal of Chemical Education*, 95(2), 197-206.

Fletcher S. (2015), "Screen-Printed Carbon Electrodes, in Electrochemistry of Carbon Electrodes," Wiley- VCH Verlag GmbH & Co., p. 425.

Hu, J., Wang, S., Wang, L., Li, F., Pingguan-Murphy, B., Lu, T. J., & Xu, F. (2014). Advances in paper-based point-of-care diagnostics. *Biosensors and Bioelectronics*, 54, 585-597.

Hutanu, F., Ocnaru, E., Arsene, M. L., & Badea-Doni, M. (2013). Screen-printed carbon electrodes modified with Prussian blue and a non-conducting electropolymerized film for selective determination of h₂o₂ in beverages. *Scientific Bulletin. Series F. Biotechnologies*, 17, 245-250.

Jensen S. "How do glucometers work?" Massachusetts Institute of Technology. [Online]. Available: <https://engineering.mit.edu/engage/ask-an-engineer/how-do-glucometers-work>.

Lin, Y., Lu, F., & Wang, J. (2004). Disposable carbon nanotube modified screen-printed biosensor for amperometric detection of organophosphorus pesticides and nerve agents. *Electroanalysis: An International Journal Devoted to Fundamental and Practical Aspects of Electroanalysis*, 16(1-2), 145-149.

Montiel, M. A., Iniesta, J., Gross, A. J., & Marken, F. (2017). Dual-plate gold-gold microtrench electrodes for generator-collector voltammetry without supporting electrolyte. *Electrochimica Acta*, 224, 487-495.

Peiris, A., & Stein, B. (2019, October 22). Capillary Action. Retrieved from [https://chem.libretexts.org/Bookshelves/Physical_and_Theoretical_Chemistry_Textbook_Maps/Supplemental_Modules_\(Physical_and_Theoretical_Chemistry\)/Physical_Properties_of_Matter/States_of_Matter/Properties_of_Liquids/Capillary_Action](https://chem.libretexts.org/Bookshelves/Physical_and_Theoretical_Chemistry_Textbook_Maps/Supplemental_Modules_(Physical_and_Theoretical_Chemistry)/Physical_Properties_of_Matter/States_of_Matter/Properties_of_Liquids/Capillary_Action).

Renub Research. (2018). Point of Care Testing Market, Global Forecast, by Diagnostics, Mode, End Users, Regions & Companies. Point of Care Testing Market, Global Forecast, by Diagnostics, Mode, End Users, Regions & Companies (pp. 0–132).

Venton, J. “Electrochemical glucometers,” University of Virginia. [Online]. Available: <http://faculty.virginia.edu/analyticalchemistry/Electrochem%20Gluc/Electrochem.html>.

Wang, S., Zhao, X., Khimji, I., Akbas, R., Qiu, W., Edwards, D., ... & Demirci, U. (2011). Integration of cell phone imaging with microchip ELISA to detect ovarian cancer HE4 biomarker in urine at the point-of-care. *Lab on a Chip*, *11*(20), 3411-3418.

Washburn, E. W. (1921). The dynamics of capillary flow. *Physical review*, *17*(3), 273.

Yetisen, A. K., Akram, M. S., & Lowe, C. R. (2013). Paper-based microfluidic point-of-care diagnostic devices. *Lab on a Chip*, *13*(12), 2210-2251.

